J_ID: Z3O Customer A_ID: 11-0317.R2 Cadmus Art: Z3O-23054 Date: 8-February-12 Stage: Page: 1

RESEARCH ARTICLE

# Anatomical Basis of Sun Compass Navigation I: The General Layout of the Monarch Butterfly Brain

Stanley Heinze,* and Steven M. Reppert

Department of Neurobiology, University of Massachusetts Medical School, Worcester, Massachusetts 01605

## ABSTRACT

Each fall, eastern North American monarch butterflies (*Danaus plexippus*) use a time-compensated sun compass to migrate to their overwintering grounds in central Mexico. The sun compass mechanism involves the neural integration of skylight cues with timing information from circadian clocks to maintain a constant heading. The neuronal substrates for the necessary interactions between compass neurons in the central complex, a prominent structure of the central brain, and circadian clocks are largely unknown. To begin to unravel these neural substrates, we performed 3D reconstructions of all neuropils of the monarch brain based on anti-synapsin labeling. Our work characterizes 21 well-defined neuropils (19 paired, 2 unpaired), as well as all synaptic regions between the more classically defined neuropils. We also studied the internal organization of all major neuropils on brain sections, using immunocytochemical stainings against synapsin, serotonin, and γ-aminobutyric acid. Special emphasis was placed on describing the neuroarchitecture of sun-compass-related brain regions and outlining their homologies to other migratory species. In addition to finding many general anatomical similarities to other insects, interspecies comparison also revealed several features that appear unique to the monarch brain. These distinctive features were especially apparent in the visual system and the mushroom body. Overall, we provide a comprehensive analysis of the brain anatomy of the monarch butterfly that will ultimately aid our understanding of the neuronal processes governing animal migration. J. Comp. Neurol. 000:000–000, 2012.



**INDEXING TERMS:** central complex; mushroom body; antennal lobes; visual system; Danaus plexippus; comparative neuroanatomy

The southward fall migration of eastern North American monarch butterflies (*Danaus plexippus*) to their overwintering grounds in central Mexico is one of the most intriguing phenomena in the animal world. In the spring, the overwintering monarchs reproduce and fly northward to the southern United States so that females can oviposit fertile eggs on newly emerging milkweed plants, the obligated food source of the larvae. A subsequent two generations of reproductively active butterflies complete the journey north to reach the northern-most range of their habitat (Reppert et al., 2010).

The fall migrants are in reproductive diapause, have an extended lifespan, and are driven to fly in a southerly direction, while the summer monarchs that give rise to the migratory generation are reproductive, have a shorter lifespan, and show nondirected flight patterns (Zhu et al., 2009). The behavioral differences between migratory and summer monarchs are partly reflected by changes in gene expression in the brain between the two states (Zhu et al., 2008). With a full set of protein-coding genes for the monarch butterfly in hand (Zhan et al., 2011), a comprehensive search for migration-specific gene expression patterns is now possible. To achieve mapping of these expression patterns to brain regions and neural circuits, a precise anatomical understanding of the monarch brain is required.

Behavioral experiments have shown that the monarch uses a time-compensated sun compass to maintain a southerly bearing during fall migration, using the sun itself and the pattern of polarized skylight as directional cues



Grant sponsor: AFOSR; Grant number: FA9550-10-1-0480; Grant sponsor: Human Frontier Science Program long-term fellowship; Grant number: LT000379/2009-L (to S.H.).

*CORRESPONDENCE TO: Stanley Heinze, University of Massachusetts Medical School, Department of Neurobiology, 364 Plantation St., Worcester, MA, 01605. E-mail: stanley.heinze@umassmed.edu

Received September 23, 2011; Revised November 14, 2011; Accepted January 20, 2012

DOI 10.1002/cne.23054

Published online Month 00, 2012 in Wiley Online Library (wileyonlinelibrary.com)



ID: sureshkumard | Black Lining: [ON] | Time: 20:29 | Path: N:/3b2/CNE#/Vol00000/120021/APPFile/JW-CNE#120021

(Perez et al., 1997; Mouritsen and Frost, 2002; Froy et al., 2003; Reppert et al., 2004). Electrophysiological recordings have revealed that neurons in the central brain respond to skylight cues with changes in firing frequency and that the central complex, a midline-spanning group of neuropils in the center of the brain, is the most likely candidate region to comprise an internal sun compass (Heinze and Reppert, 2011). As any functional sun compass needs a circadian clock to compensate for changes in solar position over the course of the day, much effort has been directed at understanding the molecular control of the monarch circadian clock and delineating its location in the brain (Reppert, 2006). Surprisingly, the major time compensation clocks for successful sun compass orientation reside in the antennae of the monarch (Merlin et al., 2009). It has been recently proposed that an additional form of time compensation is needed to ensure that all skylight information received by the sun compass system is consistent, despite the changes in solar elevation that occur over the course of the day (Pfeiffer and Homberg, 2007; Heinze and Reppert, 2011). In monarchs, this "elevation compensation" may be regulated by circadian clocks located in the pars lateralis regions of central brain (Sauman et al., 2005). Thus, there appears to be a complex interplay between antennal clocks, brain clocks, and the proposed internal compass in the central complex.

*Abbreviations*

| | |
|---|---|
| a, | Anterior |
| AL, | Antennal lobe |
| ACa, | Accessory calyx |
| AMe, | Accessory medulla |
| AMMC, | Antennomechanosensory and motor center |
| AOTu, | Anterior optic tubercle |
| Ca, | Calyx |
| CB, | Central body |
| CBL, | Lower division of the central body |
| CBU, | Upper division of the central body |
| d, | Dorsal |
| ir, | Immunoreactivity |
| l, | Lateral |
| La, | Lamina |
| LAL, | Lateral accessory lobe |
| Lb, | Lobe |
| Lo, | Lobula |
| LoP, | Lobula plate |
| LT, | Lateral triangle |
| LU, | Lower unit |
| m, | Medial |
| Me, | Medulla |
| MB, | Mushroom body |
| No, | Noduli |
| NU, | Nodular unit |
| OG, | Optic glomerular complex |
| OL, | Optic lobe |
| p, | Posterior |
| PB, | Protocerebral bridge |
| Pe, | Pedunculus |
| POTu, | Posterior optic tubercle |
| SOG, | Suboesophageal ganglion |
| SP, | Strap |
| UU, | Upper unit |
| v, | Ventral |

The central complex is present in all insects examined and is characterized by its regular, almost crystalline appearance, owing to its repetitive composition of layers and columns. It is one of the highest centers for sensory integration, and it is also involved in motor control (Strauss, 2002; Homberg, 2008). The central complex is thus well suited to serve as a major integration and staging center of the insect brain. The gross layout of the monarch central complex has been described recently (Heinze and Reppert, 2011), but little is known about its detailed neuroarchitecture, the structure of the surrounding brain, and the regions comprising its potential input and output pathways. Because the physical structure of the brain is the substrate for the interaction between gene expression and neuronal activity that ultimately defines the behavioral state of the animal, a thorough description of monarch brain anatomy is required.

In this study, we utilized recent advances in data processing and imaging techniques to provide 3D reconstructions of all regions of the monarch brain, based on whole-brain preparations. This approach, which has been used successfully in several other insect species, including the honeybee, *Apis mellifera* (Brandt et al., 2005), hawkmoth, *Manduca sexta* (el Jundi et al., 2009), red flour beetle, *Tribolium castaneum* (Dreyer et al., 2010), desert locust, *Schistocerca gregaria* (Kurylas et al., 2008), and fruit fly, *Drosophila melanogaster* (e.g., Rein et al., 2002), will allow for detailed comparisons among species. We complemented the whole-brain reconstructions with classical immunocytochemical stainings of brain sections to obtain high-resolution images of each monarch brain region. Combined, both methods provide a detailed description of the monarch brain and an anatomical reference frame for single neuron morphologies, gene expression data, expression maps of neuroactive substances, and accurate targeting for physiological recordings.

## MATERIALS AND METHODS

### Animals

Migratory and summer (nonmigratory) monarch butterflies were housed in the laboratory in glassine envelopes in Percival incubators with controlled light and temperature cycles and 70% humidity. Migrants were maintained in fall-like conditions (11 hours light at 23°C: 13 hours dark at 12°C), while nonmigrants were maintained on a lighting cycle of 12:12-hour light:dark at 25°C. Butterflies were fed a 25% honey solution every other day. Over the course of the study animals were obtained either in the wild or from commercial sources. Migrating monarch butterflies were captured in the wild while roosting. They were caught by David G. Cook at St. Mark's Wildlife refuge (near Tallahassee, FL), by Harlen E. Aschen and Altus

TABLE 1.
Primary Antibodies

| Antigen | Immunogen | Manufacturer, species, type, catalog number | Dilution used |
|---|---|---|---|
| Synapsin | Fusion protein of glutathione-S-transferase and the *Drosophila* SYN1 protein | Developed by G. Buchner (University of Würzburg, Germany), obtained from the Developmental Studies Hybridoma Bank, University of Iowa; mouse, monoclonal, 3C11 | 1:50 |
| Serotonin | Serotonin coupled to bovine serum albumin (BSA) with paraformaldehyde | Immunostar, rabbit, polyclonal, 20080, Lot 5420201 | 1:4,000 |
| GABA | GABA coupled to BSA | Sigma-Aldrich, rabbit, polyclonal, A2052, Lot 099K4822 | 1:1,000 |

Aschen near Port Lavaca, TX, or by Carol Cullar near Eagle Pass, TX. Nonmigratory butterflies were reared by and obtained from Fred Gagnon, Greenfield, MA or from Edith Smith at Shady Oak Butterfly Farm, Brooker, FL.

## Immunocytochemistry

### *Antibodies*

The anti-synapsin antibody was a monoclonal antibody raised in mouse against fusion proteins consisting of glutathione-S-transferase and the *Drosophila* SYN1 protein (SYNORF1; Klagges et al., 1996). The specificity of the antibody has been characterized by Klagges et al. (1996). It has been shown to label synaptic neuropil in a wide range of species (e.g., Brandt et al., 2005; Kurylas et al., 2008; el Jundi et al., 2009; Dreyer et al., 2010), including monarchs (Heinze and Reppert, 2011). It was obtained from the Developmental Studies Hybridoma Bank, University of Iowa, Iowa City, IA (Table 1).

The anti-5HT (serotonin) antiserum (polyclonal, raised in rabbit; Table 1) exhibits no crossreactivity to 5-hydroxytryptophan, 5-hydroxyindole, 5-hydroxy-indole-3-acetic acid, or dopamine in Bn-SA/HRP labeling assays (Immunostar, Hudson, WI; histochemical serotonin antisera specification sheet). The specificity of the anti-5HT antiserum on monarch brain sections was tested by preadsorption of the diluted antiserum (1:4,000, with 1% normal goat serum [NGS], in 0.1 M phosphate bufferered saline with 0.3% Triton X [PBT]) with different concentrations of 5HT-bovine serum albumin (BSA) conjugate (Immunostar) for 24 hours at 4°C prior to incubation of the brain sections. At a concentration of 20 μg/ml all staining was abolished, while faint residual staining was present at lower concentrations.

The anti-γ-aminobutyric acid (GABA) antibody (polyclonal, raised in rabbit; Table 1; kind gift from Scott Waddell, University of Massachusetts Medical School, Worcester, MA) was isolated from antiserum by immunospecific purification methods that remove proteins, including immunoglobulins, that do not bind specifically to GABA. It was characterized by a dot-blot immunoassay and shows positive binding to GABA and GABA/BSA, but not to BSA alone (Sigma, St. Louis, MO; GABA antisera product information sheet). The specificity of the anti-GABA antiserum on monarch brain sections was tested by preadsorption of the diluted antiserum (1:1,000, with 1% NGS, in 0.1 M PBT) with different concentrations of GABA-BSA conjugate (Gemacbio, Saint Jean d'Illac, France) for 24 hours at 4°C prior to incubation of the brain sections. At concentrations above 10 μg/ml of GABA-BSA all staining was abolished, while faint residual staining was present after preincubation with 1 μg/ml conjugate.

Additionally, the staining patterns we obtained in monarch brain using the antibodies against serotonin or GABA were highly similar to the staining patterns in other lepidopterans (e.g., Homberg et al., 1987; Homberg and Hildebrand, 1989; Dacks et al., 2006; Berg et al., 2009).

### *Immunocytochemistry in wholemount preparations*

Two slightly different staining protocols were used to perform immunolabeling in wholemount preparations of the monarch butterfly brain. Both methods differed in the fixative and the method for permeabilization of the tissue, but shared all other steps.

Before dissection, the animals were briefly cooled on ice, decapitated, mounted in a small dish using wax, and covered in ice-cold HEPES-buffered saline (HBS; 150 mM NaCl; 5 mM KCl; 5 mM $CaCl_2$; 25 mM sucrose; 10 mM HEPES (N-[2-hydroxyethyl]piperazine-N′-[2-ethanesulphonic acid]) (Ott, 2008). The brain was dissected out of the head capsule within 10 minutes and immediately transferred into the fixative. This was either 4% paraformaldehyde (PFA) in 0.1 M phosphate-buffered saline (PBS, pH 7.4), or Zn-FA fixative (0.25% [18.4 mM] $ZnCl_2$, 135 mM NaCl, 35 mM sucrose, 1% PFA) (Ott, 2008). After the brain was freed of trachea and fatbody, the retina was carefully removed from the lamina with a pair of scissors. Fixation lasted 2 hours at room temperature (for PFA) or 20 hours at room temperature (for Zn-FA). The brains were then washed in HBS (8 × 25 minutes; Zn-FA protocol) or in PBS (4 × 15 minutes; PFA protocol). For permeabilizing the tissue, the brains were either incubated in a mixture of methanol and dimethyl sulfoxide (DMSO) (ratio 20:80, 90 minutes; Zn-FA protocol) or



ID: sureshkumard | Black Lining: [ON] | Time: 20:29 | Path: N:/3b2/CNE#/Vol00000/120021/APPFile/JW-CNE#120021

incubated with collagenase-dispase (60 minutes, 1 mg/ml, Roche, Nutley, NJ; PFA-protocol). Brains were rinsed in 0.1 M Tris-buffer (3 × 10 minutes; Zn-FA protocol) or 4 × 15 minutes in PBT at room temperature.

All remaining steps were identical for both protocols. Preincubation was performed by incubating the brains with 5% NGS (in 0.1 M PBT) overnight at 4°C. The primary antibody (anti-synapsin) was applied for 5 days at 4°C at a concentration of 1:50 (with 1% NGS in 0.1 M PBT). Thereafter, brains were intensely rinsed (8 × 25 minutes in PBT) before the secondary antibody was applied (DyLight647-conjugated goat antimouse, 1:300; with 1% NGS in 0.1 M PBT; Jackson Immunoresearch, West Grove, PA) for 3 days at 4°C. The antibody incubation was followed by intense washing steps (6 × 25 minutes 0.1 M PBT, 2 × 25 minutes 0.1 M PBS) before dehydration of the brains was achieved with an increasing ethanol series (25%, 50%, 70%, 90%, 95%, 100%; 15 minutes each). The brains were transferred to a fresh mixture of methylsalicylate and ethanol (1:1) for 15 minutes. During that time ethanol was allowed to evaporate and a smooth transition to pure methylsalicylate was ensured. Pure methylsalicylate was applied for another 35 minutes for clearing of the tissue. Last, the brains were embedded in Permount (Fisher Scientific, Pittsburgh, PA) between two glass coverslips. Spacer rings were used to prevent squeezing of the brains.

The PFA protocol led to excellent results for peripheral tissues like antennal lobes and calyces, while not allowing optimal penetration of the antibody to central regions. The Zn-FA protocol allowed optimal penetration and equal staining throughout the brain, but led to increased background in the brain periphery, making it somewhat difficult to identify peripheral neuropil boundaries clearly in some cases. All 3D reconstructions are based on the Zn-FA protocol with the exception of the high-resolution antennal-lobe reconstruction and the reconstruction of the accessory calyx.

### *Immunocytochemistry in sections*

Brains were dissected as described for wholemount preparations except that the retina was left intact. Fixation was carried out with Zamboni's fixative (4% PFA, 7.5% picric acid in 0.1 M phosphate buffer [PB], pH 7.4) for 2.5 hours at room temperature. After washing the brains in 0.1 M PB (3 × 15 minutes) they were embedded in albumin-gelatin (4.8% gelatin and 12% ovalbumin in demineralized water) and postfixed in 4% formaldehyde solution (in 0.1 M PB). The brains were then cut into 30-μm thick sections using a vibrating blade microtome (Leica VT1200, Wetzlar, Germany). The floating sections were rinsed with 0.1 M PBS (3 × 10 minutes) and incubated with 5% NGS (or natural donkey serum [NDS], depending on the species in which the secondary antibody was raised; Jackson Immunoresearch) for 1 hour at room temperature (in 0.1 M PBT). The primary antibody was applied overnight at room temperature (anti-synapsin: 1:50; anti-serotonin: 1:4,000; anti-GABA: 1:1000; Table 1) together with 1% NGS/NDS in 0.1 M PBT. After rinsing the sections with PBS (6 × 10 minutes), the secondary antibodies were added (DyLight488-conjugated goat antimouse, DyLight549-conjugated donkey antirabbit; Jackson Immunoresearch). Incubation lasted 2 hours at room temperature with 1% NGS/NDS in 0.1 M PBT. Next, the sections were rinsed in PBT (4 × 10 minutes) and PBS (2 × 10 minutes), after which they were mounted on chrome-alum/gelatin-coated glass slides. After drying overnight, the mounted sections were dehydrated in an increasing ethanol series (water, 5 minutes; 50%, 70%, 90%, 95%, 100% [twice], 3 minutes each), cleared in Xylene (2 × 5 minutes), and embedded in Entellan (EMS, Hatfield, PA).

## Neurobiotin fills

Labeling of neurons using neurobiotin as tracer was either achieved via intracellular recordings (in the case of central body tangential neurons) or as antennal backfills. During intracellular recordings (performed as described in Heinze and Reppert, 2011) a depolarizing current (0.5–3 nA) was continuously applied at the electrode (tip filled with 4% neurobiotin; Vector Laboratories, Burlingame, CA) for up to 3 minutes, after which the brain was dissected. For antennal backfills, the animal was immobilized in a plastic holder, the head was fixed with clay, and the antenna was cut shortly distal of its base. A capillary filled with 4% neurobiotin (in 1 M KCl) was slipped over the remaining antennal flagellum and left in place for 3 days, while the animal was kept at 4°C in a humidified environment. Then the brains were dissected from the head capsule as described for wholemount preparations. All neurobiotin-filled brains were rinsed in 0.1 M PBS (4 × 15 minutes) and incubated with Cy3-conjugated streptavidin (Rockland, Gilbertsville, PA) for 3 days (1:1,000, in 0.1 M PBT, 4°C). Brains were washed in PBT (4 × 20 minutes) and PBS (2 × 20 minutes) and dehydrated, cleared, and embedded as described for wholemount immunolabeling.

## Confocal imaging

All imaging was performed with a confocal laser scanning microscope (Zeiss LSM 5 Pascal). For 3D reconstructions, wholemount preparations were either imaged at low resolution using a 10× objective (Plan Neofluar 0.3; Zeiss) or at high resolution using a 25× objective (LD LCI Plan-Apochromat 25×/0.8 Imm Corr DIC; Zeiss). To cover the whole brain or details of larger structures in the central brain, up to 12 image stacks had to be acquired

from anterior and posterior. These were aligned and merged afterwards either using the ImageJ implementation FIJI (general public license, downloadable from http://fiji.sc) or Amira5.2 software (Mercury Computer Systems, San Diego, CA). Low-resolution scans were resampled to a final voxel size of 3 $\mu m^3$, while high-resolution scans were resampled to a final voxel size of 1 $\mu m^3$ (most reconstructions) or 2 $\mu m^3$ (for complete reconstruction of the central brain only). As cubic voxels are desirable for reconstruction in Amira and the resolution of the acquired image stacks was limited in the z-direction, smaller voxel sizes were not achievable with the objectives used. Additionally, only resampling allowed processing of the otherwise very large data stacks with the given computational capabilities.

Detailed images of brain sections were acquired using either one of the following objectives: 10× air (see above), 25× oil immersion (see above), or 63× oil immersion (Plan Apochromat 1.4 oil; Zeiss). Stacks were scanned with 1024 × 1024 voxels with optical sections every 1 μm (for high magnifications). Overview scans with 10× objective were achieved with a single scan, not an image stack. In case several images were needed to cover a structure of interest, they were acquired separately and afterwards merged with FIJI. For scans of double-labeled preparations, the separate channels were always scanned sequentially, not simultaneously, to avoid bleed-through artifacts. Different color maps were allocated to individual channels irrespective of the original fluorophore color. Images of serotonin immunostaining are presented monochrome and inverted for better reproduction of fine details in printed figures. Most images shown were optimized for brightness and contrast. Unless stated otherwise, all confocal images are single optical sections.

### Three-dimensional reconstructions

All neuropil reconstructions were based on anti-synapsin-labeled wholemount preparations. After the image stacks that contained a particular neuropil of interest had been aligned, merged, and resampled (see above), the resulting combined image stack was used as the basis for reconstruction in Amira5.2. For images obtained with the 10× air objective, the mismatch of refractive indices leading to artificially shortened z-dimensions had to be corrected. The correction factor was calculated by scanning the identical structure with the 10× air objective and the 25× oil immersion objective and comparing the z-dimensions of both scans (result: 1.49).

For reconstructions, the segmentation editor of Amira was used to create a volumetric dataset called labelfield, in which voxels of the image stack were assigned to particular neuropil structures. This was achieved by manually assigning key sections in all three spatial planes to a neuropil and using the wrapping function of Amira to interpolate the complete structure. This segmentation process was repeated for all neuropils of interest located in the current image stack. After all neuropils were completed, a polygonal surface model was automatically calculated. The color code used for neuropils was based on the standard brains of the honeybee, the hawkmoth, the desert locust, and *Tribolium castaneum* (Brandt et al., 2005; Kurylas et al., 2008; el Jundi et al., 2009; Dreyer et al., 2010). Volumes of neuropils were calculated from label fields using the tissue-statistics tool in Amira.

## RESULTS

### General layout of the monarch butterfly brain

The general layout of the monarch butterfly brain was analyzed with anti-synapsin immunolabeling in whole-brain preparations combined with 3D reconstructions of all identifiable brain areas based on confocal images.

The brain of the monarch butterfly is composed of the central brain and, located on either side, the large optic lobes (Fig. 1). It is connected to the thoracic ganglia and the remaining ventral nerve cord through the neck connective emerging ventrally. Each optic lobe is directly adjacent to the retina of the compound eye and connected to the central brain via the optic stalk. Generally, the coordinates of the brain are defined both by the neuraxis and the body axis, which are roughly at 90° angles with respect to one another. For reasons of simplicity and due to the fact that during development the neuraxis undergoes substantial distortions and rotations (Huetteroth et al., 2010), all coordinates in this work refer to the body axis of the animal. F1

As in other lepidopterans and many other insects, the monarch brain is a fusion product of the supraoesophageal ganglion (SPG) and the suboesophageal ganglion (SOG), which engulf the medially transecting oesophagus between them (Fig. 1A,B,D–G). Developmentally, the SOG is a fusion of the mandibular, maxillary, and labial neuromeres. The SPG consists of the protocerebrum, deutocerebrum, and tritocerebrum, whose neuromere identities are still controversial. The boundaries between these regions could not be distinguished easily and will thus be disregarded in the following sections. As in all insects, the somata of monarch neurons are located in the peripheral regions of the brain, the cell body rind, whereas all neuronal connections are made in the neuropil regions in the inner areas of the brain. Within the neuropil, a distinction can be made between synaptic neuropil, which contains the vast majority of synapses, and fibrous neuropil, which comprises all tracts, fiber bundles, commissures,

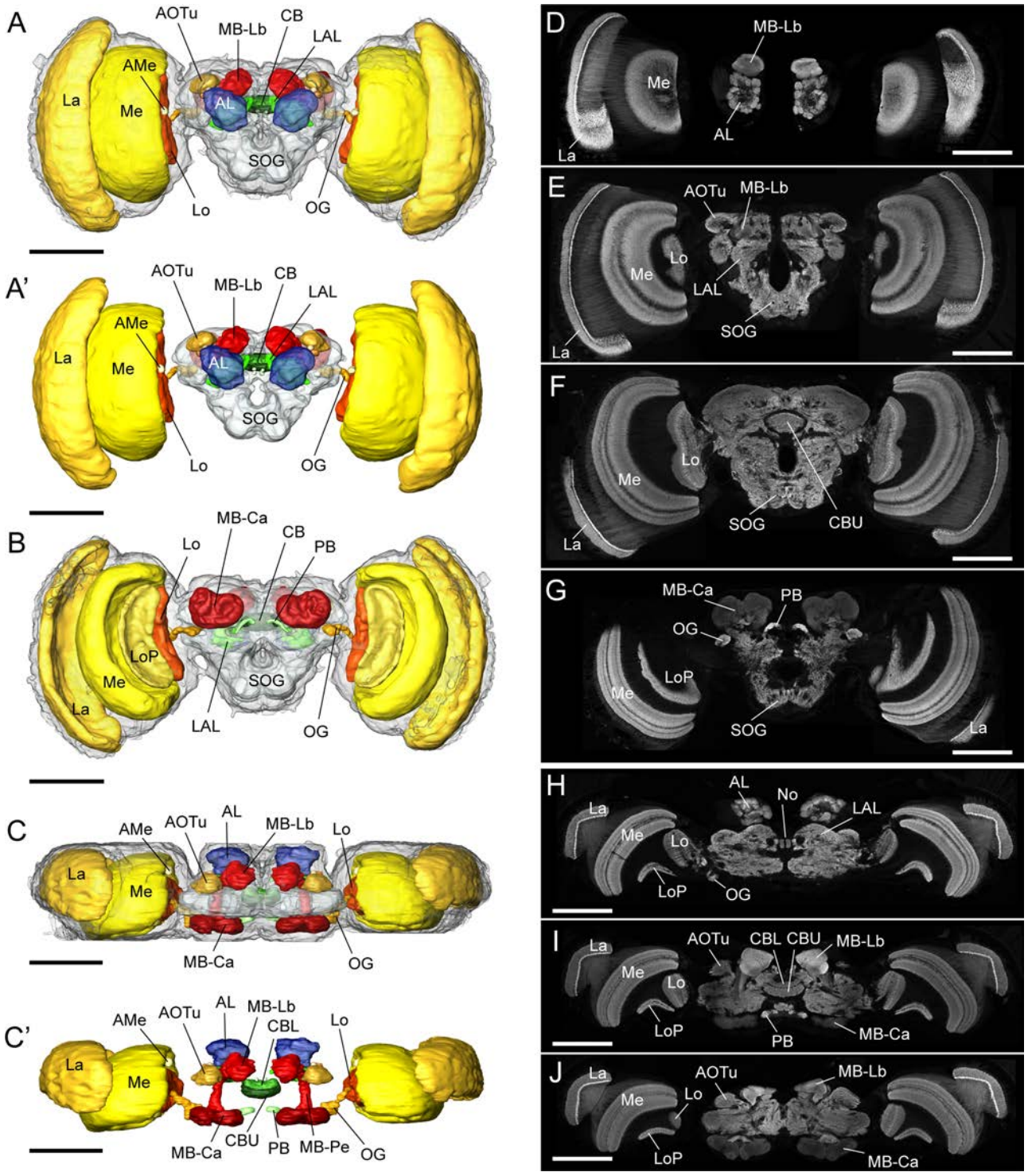


COLOR

Figure 1. Overview of the anatomical organization of the monarch butterfly brain. **A:** Anterior view of 3D reconstruction of the monarch brain based on synapsin-ir in a wholemount preparation. Defined neuropils are represented in false colors, unspecified neuropils are shown in gray, while the surface of the brain is shown as transparent envelope. **A′:** Identical to A, but without visualization of the brain surface, to illustrate the limits of synaptic labeling. **B:** Posterior view of 3D brain reconstruction. **C:** Dorsal view of the reconstructed monarch brain. **C′:** Identical to C, but with brain surface and unspecified neuropils removed for clarity. **D–G:** Confocal images of anti-synapsin labeled frontal vibratome sections (thickness, 30 μm) at different levels through the monarch butterfly brain from anterior (D) to posterior (G). **H–J:** Like D–G, but sections were cut in the horizontal plane. Sections range from ventral to dorsal regions of the supraoesophageal ganglion. Scale bars = 500 μm.

and fiber chiasmata, all of which serve as connections between different synaptic neuropils.

In monarch brain, anti-synapsin labeled only synaptic neuropil, leaving fiber bundles as dark holes or occasionally as faint, nonspecific background staining. Overall, 21 synaptic neuropil areas were distinguished unambiguously, two of which were unpaired, whereas all remaining ones occurred on both sides of the midline. These defined neuropils contained ≈82% of all synaptic neuropil. The remaining unspecified neuropil, in fact the largest portion of the central brain, occupied the space between the defined regions but lacked distinct boundaries. Therefore, these regions were subdivided according to their location relative to brain landmarks such as fiber bundles, and according to their appearance in anti-synapsin-labeled preparations (e.g., dense and smooth vs. coarse). Accordingly, the unspecified neuropil regions could be divided into five major areas (details see below).

## Optic lobes

Following the path that retina-sensed skylight cues take through the monarch brain, we first examined the optic lobes. Combined, the two optic lobes comprise about 74% of the total brain volume and consist of five major neuropils. From distal to medial, we identified the lamina, which is directly adjacent to the retina, the medulla, and the lobula. These three structures form a stack of convex neuropils in which the outer ones partly engulf the inner ones (Fig. 2A–D). Prominently located between the lamina and the medulla is the first optic chiasma, the massive anterior–posterior fiber crossing, in which projections from lamina cartridges connect to their target medulla columns (Fig. 2E), whereas the second optic chiasma is located between the medulla, lobula, and the lobula plate. The lobula plate, the fourth neuropil of the optic lobe, is a thin, slightly convex plate, located posterodorsally of the lobula. The accessory medulla, a small, spherical neuropil, is located anterior of the lobula, on the medial edge of the medulla (Fig. 2). F2

More detailed observation revealed that the monarch lamina is characterized by an unusual inner rim, which showed bright synapsin-immunoreactivity (-ir) (Fig. 2E–G). Furthermore, the medulla could be divided into an inner and an outer division, separated by the serpentine layer, in which large fibers, presumably from tangential neurons, were found (Fig. 2E–J). Based on synapsin-ir, the outer medulla was composed of six distinct layers of different width. The inner medulla contained three layers, which were less sharply separated from each other (Fig. 2I). While stratification was not as clearly defined as in the medulla, the lobula plate was divided into three layers (Figs. 1H–J, 2E), and the lobula was separated into an outer and an inner division.

Interestingly, there was another small neuropil area consistently found in the optic lobe, just anterior of the accessory medulla (Fig. 2J–N). From the midline, this thin strip of irregularly shaped neuropil runs ventrally alongside the medial edge of the medulla and merges on its dorsal edge with the accessory medulla.

## Anterior optic tubercles

The first processing stage for skylight information in the central brain of the monarch is the anterior optic tubercle (AOTu) (Heinze and Reppert, 2011). This group of neuropils is located just below the anterior surface of the brain and occupies the dorsolateral part of the anterior protocerebrum. The AOTu could be divided into a large upper unit and a number of smaller units: the lower unit, the nodular unit, and the strap (Fig. 3). The anterior-most located lower unit is a spherical neuropil of uniform, dense appearance when labeled against synapsin. The posterior edge of the lower unit merges into an elongated, rather irregular structure called the strap. The strap bends ventrolaterally toward the nodular unit and has a much coarser, yet intensely stained appearance (Fig. 3D,E). Clustered around the elongated end of the strap are the three components of the nodular unit. Each of them possesses a rounded, tube-like shape, extending laterally toward the optic stalk. Located just posterior of the lower unit, but dorsal of the strap, is the first compartment, while the second and third can be found ventral of the strap, stacked on top of each other (Fig. 3A–F). The appearance of the synapsin labeling varied between the different nodular unit components and even within individual compartments, suggesting further specializations within this complex structure. F3

The upper unit of the AOTu is massively enlarged compared with the remaining units and had a uniformly coarse, sponge-like structure (Fig. 3F–H). It occupies the space between the optic lobe (laterally), the mushroom body lobe system (medially), and the ventrolateral protocerebrum (ventrally) and extends posteriorly down to the level of the central body, where it lies adjacent to the superior lateral protocerebrum.

## Lateral accessory lobes

The lateral accessory lobes (LAL) are located on either side of the central body and can be divided into four divisions: the large dorsal and ventral LAL, a small anterior division (anterior loblet), and the lateral triangle (Fig. 4). They are intimately linked to the central complex and, as in the desert locust, appear to provide a relay between different AOTu-compartments and specific subunits of the central body, thus being crucially involved in processing skylight compass cues (Pfeiffer et al., 2005; Heinze and Reppert, 2011). F4

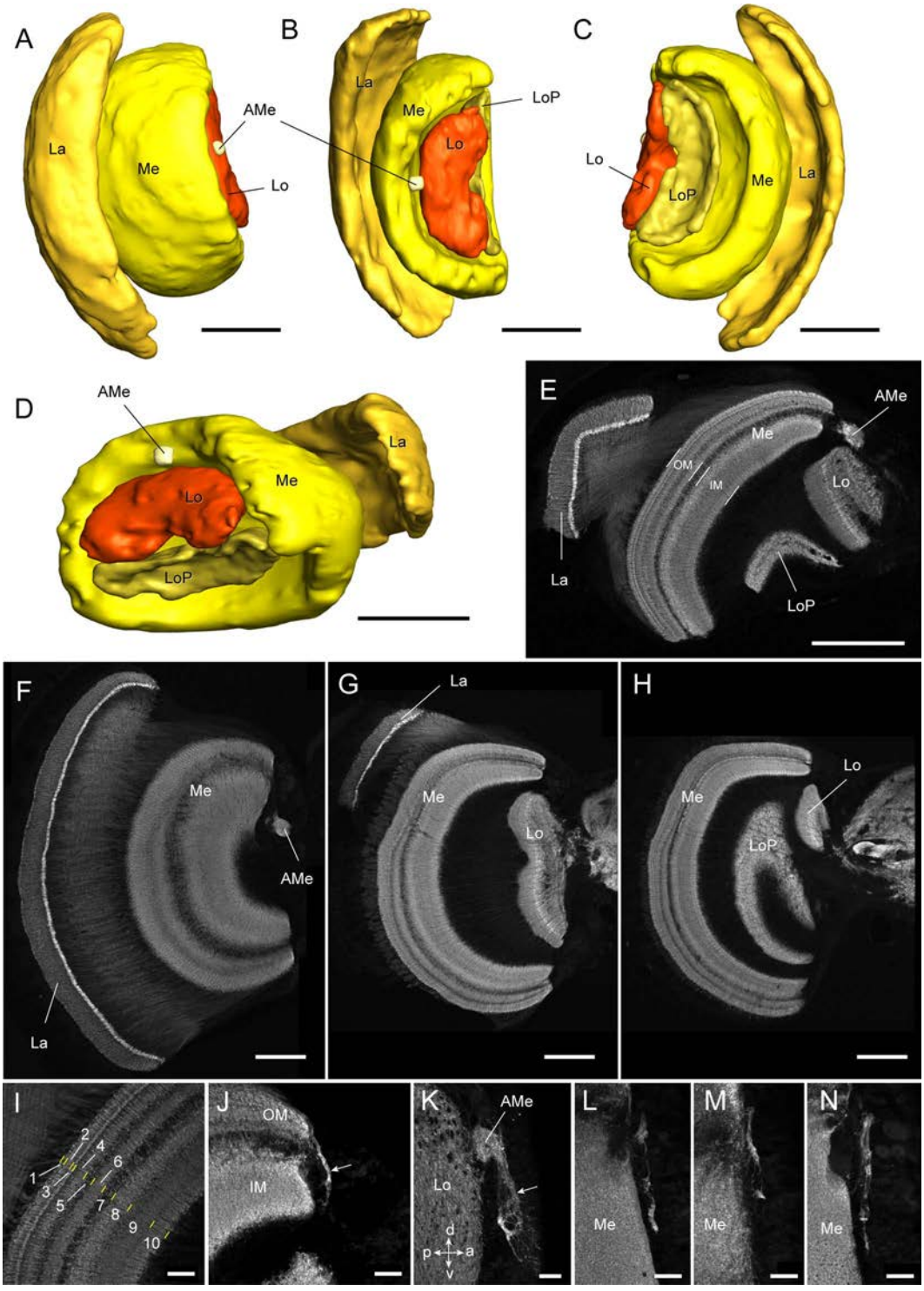


COLOR

Figure 2. Anatomical organization of the optic lobes. **A–D:** 3D reconstruction of the optic lobe neuropils based on synapsin-ir in a wholemount preparation (A: anterior view; B: medial view; C: posterior view; D: oblique view). **E:** Confocal image of a horizontal section of the optic lobe stained against synapsin (thickness, 30 μm). The section reveals the relative location of all major optic lobe neuropils, the first optic chiasm, as well as the separation of the medulla into outer and inner medulla. **F–H:** Confocal images (maximal intensity projections; stepsize: 3 μm; depth: 6–8 images) of frontal vibratome sections (thickness, 30 μm) of an anti-synapsin-labeled optic lobe. Note the bright inner rim of the lamina and the prominent stratification of the medulla (F–H, anterior to posterior). **I:** Detail of a horizontal section of the medulla revealing the elaborate layering of this neuropil. The 10 layers were defined based on appearance of synapsin-ir. **J–N:** Irregularly shaped neuropil at the anterior, medial edge of the optic lobe (highlighted by arrow in J and K). Confocal images of horizontal (J, single optical section), sagittal (K, maximal intensity projection; depth: 17 images; stepsize 1 μm), and frontal (L–N: three different levels from anterior to posterior, maximal intensity projection; depth: 14–16 images; stepsize: 1 μm) sections stained against synapsin. Scale bars = 300 μm in A–E; 200 μm in F–H; 50 μm in I–N.

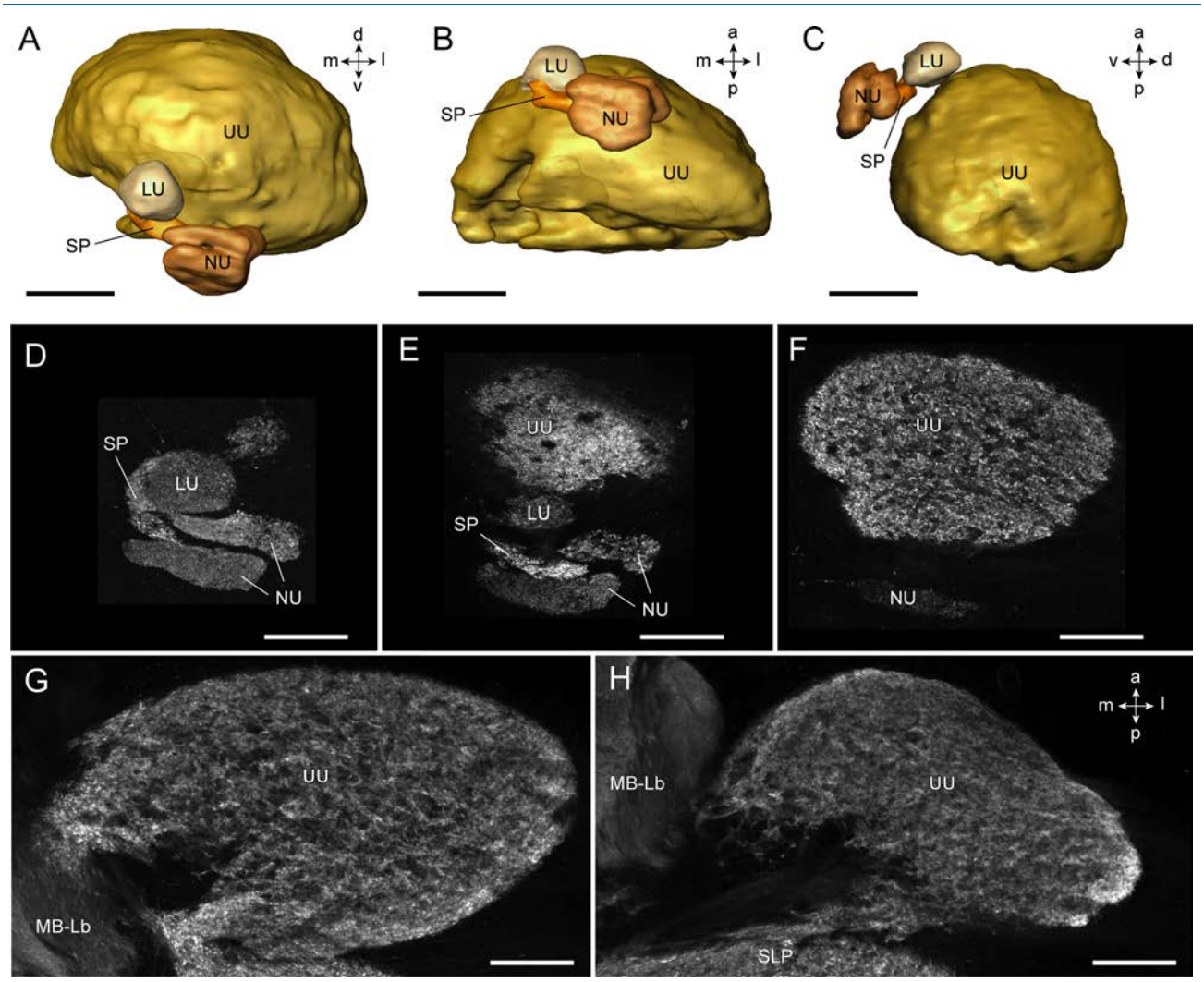


COLOR

**Figure 3.** Anatomical organization of the anterior optic tubercle. **A–C:** 3D reconstruction of an anti-synapsin-labeled anterior optic tubercle with all four subdivisions (left brain hemisphere). Shown are the upper division, the lower division, the nodular division, and the strap (A: anterior view; B: ventral view; C: lateral view). **D–G:** Confocal images of frontal vibratome sections of the left anterior optic tubercle at different levels (D–G: levels from anterior to posterior; D,E: maximal intensity projections; depth: 31 images, stepsize: 0.5 μm (D); depth: 7 images, stepsize: 1 μm (E)). All images are shown at the same scale. Note the distinct appearance of the different subunits with respect to density and intensity of synapsin-ir. **H:** Confocal image of a horizontal section of the upper unit of the anterior optic tubercle. Scale bars = 50 μm.

The LALs are clearly delineated only on their anterior sides. They occupy the region in the brain just posterior of the antennal lobes (Fig. 4F). Dorsally, they are bordered by the mushroom body lobes, the pedunculus, and the isthmus tract. While they merge with the ventrolateral protocerebrum on the lateral side, the same occurs with the posterior lateral protocerebrum ventrally and the ventromedial protocerebrum posteriorly (Fig. 4J,K). Two neuropil bridges are contiguous with the inferior protocerebrum on the dorsomedial side, anteriorly and posteriorly of the isthmus tract. This lack of clear boundaries of the monarch LAL is characteristic for this structure and has been described in other species as well (Otsuna and Ito, 2006; el Jundi et al., 2009; Iwano et al., 2010). To define these boundaries for the monarch brain, we adopted landmarks used in moths (Fig. 4D,E) (Iwano et al., 2010). Thus, the posterior limit of the LAL was defined by the mediolateral antennocerebral tract, which ventrally crosses the region from medial to lateral, as well as by the tubercle-LAL tract, which dorsally enters the region posterior of the lateral triangle. Medially, the medial antennocerebral tract provided a clear limit to the LAL, while dorsally no neuropil that extended beyond the dorsal limits of the isthmus tracts was included. To define the ventral and lateral boundaries of the LAL, anti-serotonin labeling was performed. The ventral boundary was clearly visible as the furthest extent of serotonin-immunoreactivity commissural neurons that connect the ventral parts of both LALs. The lateral boundary



ID: sureshkumard | Black Lining: [ON] | Time: 20:29 | Path: N:/3b2/CNE#/Vol00000/120021/APPFile/JW-CNE#120021

was defined by a diagonal line marked by the limit of serotonin-immunoreactivity fibers originating from the central body and the limits of fibers arborizing in the ventrolateral protocerebrum.

The lateral triangles are the most distinct LAL subdivisions and were identified as small structures on either side of the lower division of the central body (CB), to which they are connected by the isthmus tracts

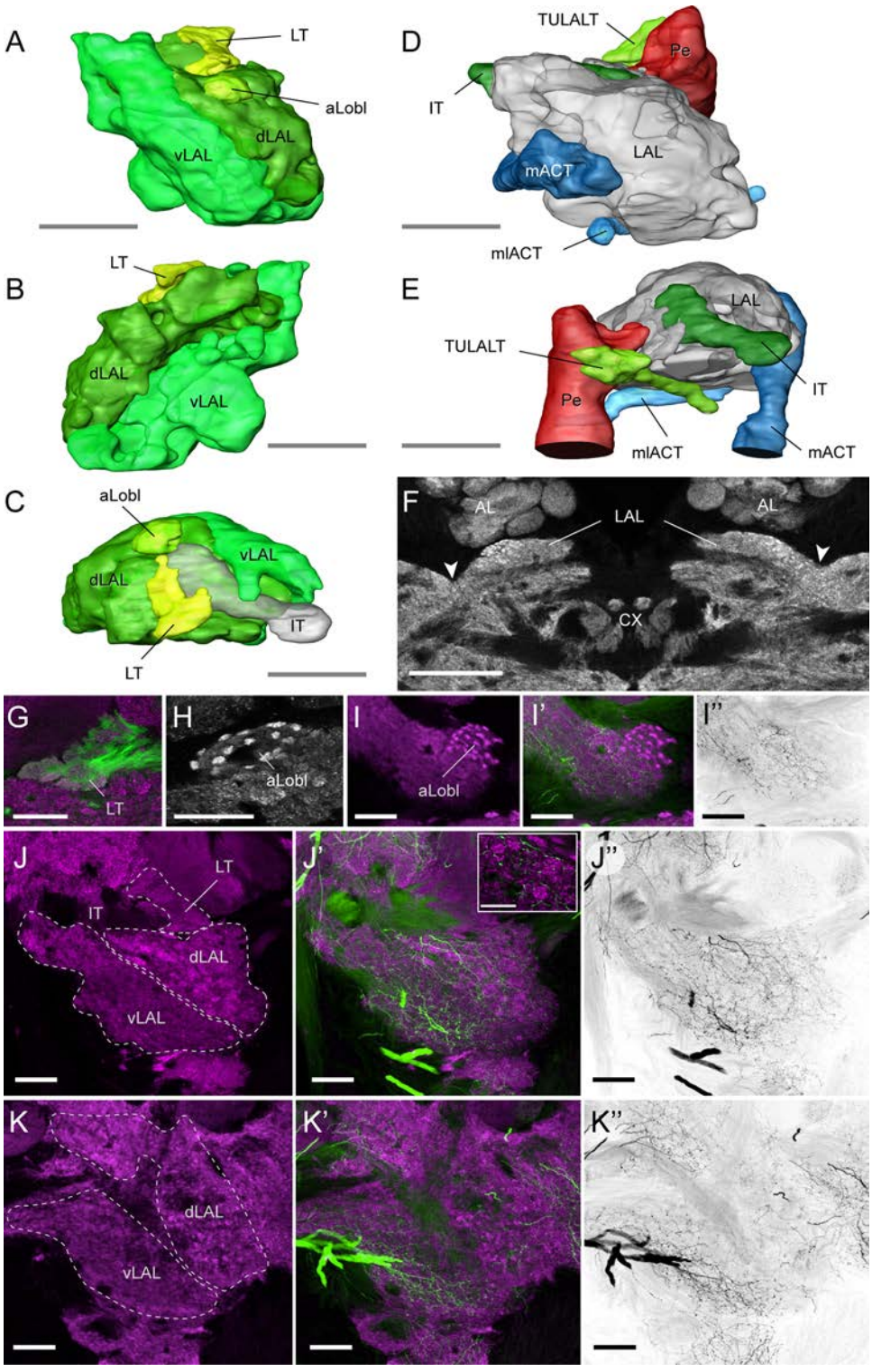


Figure 4



ID: sureshkumard | Black Lining: [ON] | Time: 20:30 | Path: N:/3b2/CNE#/Vol00000/120021/APPFile/JW-CNE#120021

(Fig. 4A–C,G). Capping the ends of these tracts, they appeared to be pressed against the medial flank of the mushroom body lobes, from which they could be easily distinguished because of a much less dense appearance. Toward the anterior end, the lateral triangles fade out as a thin sheet, whereas they are much more bulbous toward the posterior side, where they are embedded in a fiber bundle originating from the AOTu (the tubercle-LAL tract). Ventrally, they seemed to merge with the dorsal LALs and could be only distinguished when colabeled against GABA (Fig. 4G). Staining against the inhibitory transmitter GABA was highly concentrated in the lateral triangles and the isthmus tracts.

Unlike the lateral triangle, the three remaining subdivisions of the LAL were much more contiguous and could be distinguished only with the help of serotonin-ir and high-resolution images of synapsin-ir (Fig. 4A–C,H–K). First, the dorsal LAL, located dorsolaterally of the dividing LAL commissure, was characterized by a rough, glomerular appearance of synapsin-ir, and is innervated by serotonin-immunoreactivity fibers originating from the central body (Fig. 4J). These serotonin-immunoreactivity fibers are predominantly present in the anterior regions of the dorsal LAL and become sparse toward its posterior end. Second, the ventral LAL, located ventromedially of the dividing LAL commissure, possessed a smooth structure and is innervated by commissural serotonin-immunoreactivity fibers throughout (Fig. 4J,K). Third, a small structure on the very anterior limit of the LAL was characterized by bright, well-defined, nonoverlapping microglomeruli, in which almost all synapsin-ir was concentrated, and which largely lacked serotonin-ir (Fig. 4H,I). This LAL subunit has, to our knowledge, not been reported in other species, and was termed the anterior loblet of the LAL.

## Central complex

The central complex is the major integration site for skylight compass cues in monarchs, locusts, and likely crickets (Vitzthum et al., 2002; Sakura et al., 2008; Heinze et al., 2009; Heinze and Reppert, 2011). It is characterized by its intricate neuroanatomical organization of vertical columns and intersecting, horizontal layers. As in other insects, the monarch central complex is composed of a group of four neuropils: the upper and lower division of the central body (CBU and CBL), the protocerebral bridge (PB), and the paired noduli (Figs. 5–7). The two divisions of the central body are the only unpaired neuropils of the monarch brain. They are located in the center of the protocerebrum, flanked by the LALs and the inferior protocerebrum on either side. The sausage-shaped CBL lies just anterior of the larger CBU (Fig. 5). Anterior of the CBL lies a plexus of midline crossing fibers, the anterior chiasma, which gives rise to the isthmus tracts connecting the central body with the LALs and the lateral triangles. Posteriorly, the central body is separated from the PB by the posterior chiasma and a midline-crossing portion of the posterior medial protocerebrum. F5-F7

The PB itself consists of two separate, tubular neuropils on either side of the midline, which are connected by a large commissure. While extending laterally away from the midline, each half subsequently bends ventrally, but remains in the same frontal plane (Fig. 7E,F). The eight segments that each half of the PB consists of are largely fused and can only be distinguished close to the lateral ends; particularly the last segment is clearly distinct from the rest of the PB. The four fiber bundles generally connecting the central body and the PB (from lateral to medial: w-, x-, y-, and z-bundles [Williams, 1975]) are confined within two gaps present in the unspecified neuropils

**Figure 4.** Anatomical organization of the lateral accessory lobes. **A–C:** 3D reconstruction of the lateral accessory lobe (LAL) based on synapsin-ir in a wholemount preparation. Shown are the subdivisions of the LAL (dorsal LAL, dLAL; ventral LAL, vLAL; anterior loblet, aLobl; and lateral triangle, LT), as well as the isthmus tract (IT) in C (A: anterior view; B: posterior view; C: dorsal view). **D,E:** Visualization of the fiber tracts used to define the boundaries of the LAL (shown in gray); anterior view (D) and oblique dorsoposterior view (E). Tracts were reconstructed based on synapsin-ir (i.e., faint, fibrous background staining in regions without synaptic neuropil as opposed to bright synaptic labeling). The posterior boundary was defined by the mediolateral antennocerebral tract (mlATC) and the tubercle-LAL-tract (TULALT), while the medial and dorsal boundaries were defined by the medial antennocerebral tract (mACT) and the IT (together with the pedunculus of the mushroom body), respectively. **F:** Confocal image of a horizontal brain section stained against synapsin, revealing the general location of the LALs with respect to the antennal lobes (AL) and the central complex (CX). Arrowheads indicate contiguous neuropil between the LAL and the ventrolateral protocerebrum. **G:** Single optical section of a confocal image stack stained against GABA (green) and synapsin (magenta), showing the LT (frontal vibratome section). Note that GABA-ir is restricted to the LT without labeling the surrounding neuropils. **H:** Single optical section of a confocal image stack stained against synapsin (horizontal vibratome section), showing the fine structure of the aLobl with its microglomerular appearance. **I–K:** Maximal intensity projections (depth: 10 images (I), 17 images (J,K); stepsize 1 μm) of confocal image stacks stained against serotonin (green in (′), black in (″)) and synapsin (magenta). Shown are frontal vibratome sections at three levels of the LAL (I to K, anterior to posterior), (I–K) synapsin-ir, (**I″–K″**) serotonin-ir (inverted, monochrome for enhanced visibility), and (I′–K′) superposition of both. Inset in J′ illustrates microglomerular structure of the dLAL at high resolution. Scale bars = 100 μm in A–E; 200 μm in F; 50 μm in G–K; 20 μm in inset J′.

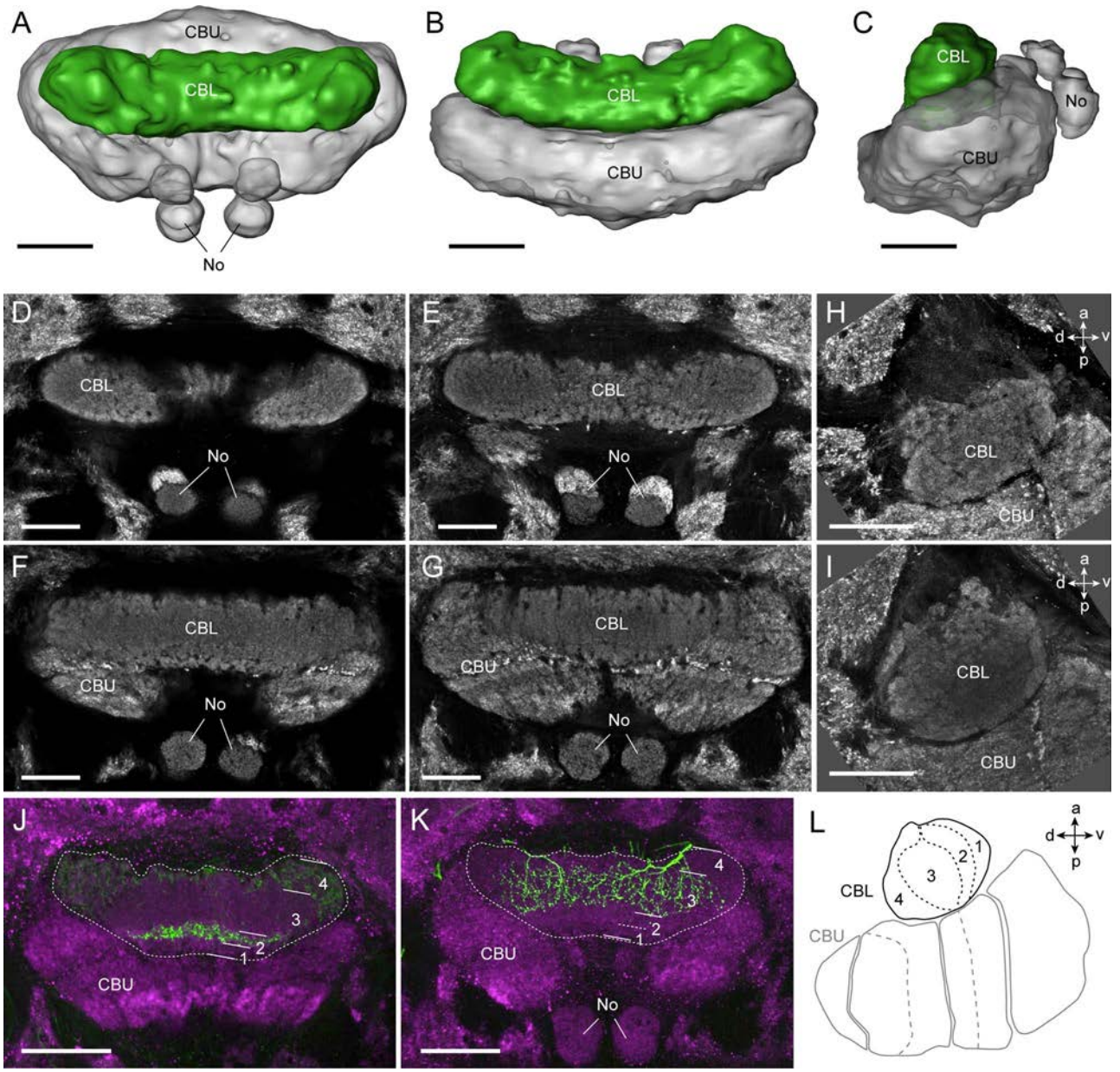


COLOR

**Figure 5.** Anatomical organization of the lower division of the central body. **A–C:** 3D reconstruction of the central body (including the noduli, No) based on synapsin-ir in a wholemount preparation. The lower division of the central body (CBL) is shown in green, while the rest of the central complex structures are shown in gray (A: anterior view; B: dorsal view; C: lateral view). **D–G:** Confocal images of frontal vibratome sections stained against synapsin, illustrating the dense appearance of the CBL (D–G, anterior to posterior). **H,I:** Confocal images (maximal intensity projections; depth: 5 images (H), 3 images (I); stepsize 1 μm) of sagittal sections stained against synapsin showing the CBL in cross-section (H: medial section; I: lateral section). **J,K:** Confocal images (maximal intensity projections; depth: 6 images (J), 14 images (K); stepsize 1 μm) of colabeling of synapsin-ir (magenta) and neurobiotin injected neurons originating from the lateral triangle. Arborizations of the injected neurons are confined to specific regions of the CBL allowing the identification of four dorsoventral layers. **L:** Schematic illustration of CBL-layers as revealed by neurobiotin injections (sagittal view). Scale bars = 50 μm.

that separate the central body from the PB. The larger one is located medially and contains neurons belonging to the three medial bundles, as well as the medial antennocerebral tract, while the lateral, smaller gap contains neurons belonging to the w-bundle (Heinze and Reppert, 2010).

As the last component of the central complex, the noduli are located just ventral of the central body on either side of the midline. They consist of an upper and lower part, each of which can be further divided into two compartments, so that both noduli are composed of four compartments arranged in a roughly linear stack from anterior



ID: sureshkumard | Black Lining: [ON] | Time: 20:30 | Path: N:/3b2/CNE#/Vol00000/120021/APPFile/JW-CNE#120021

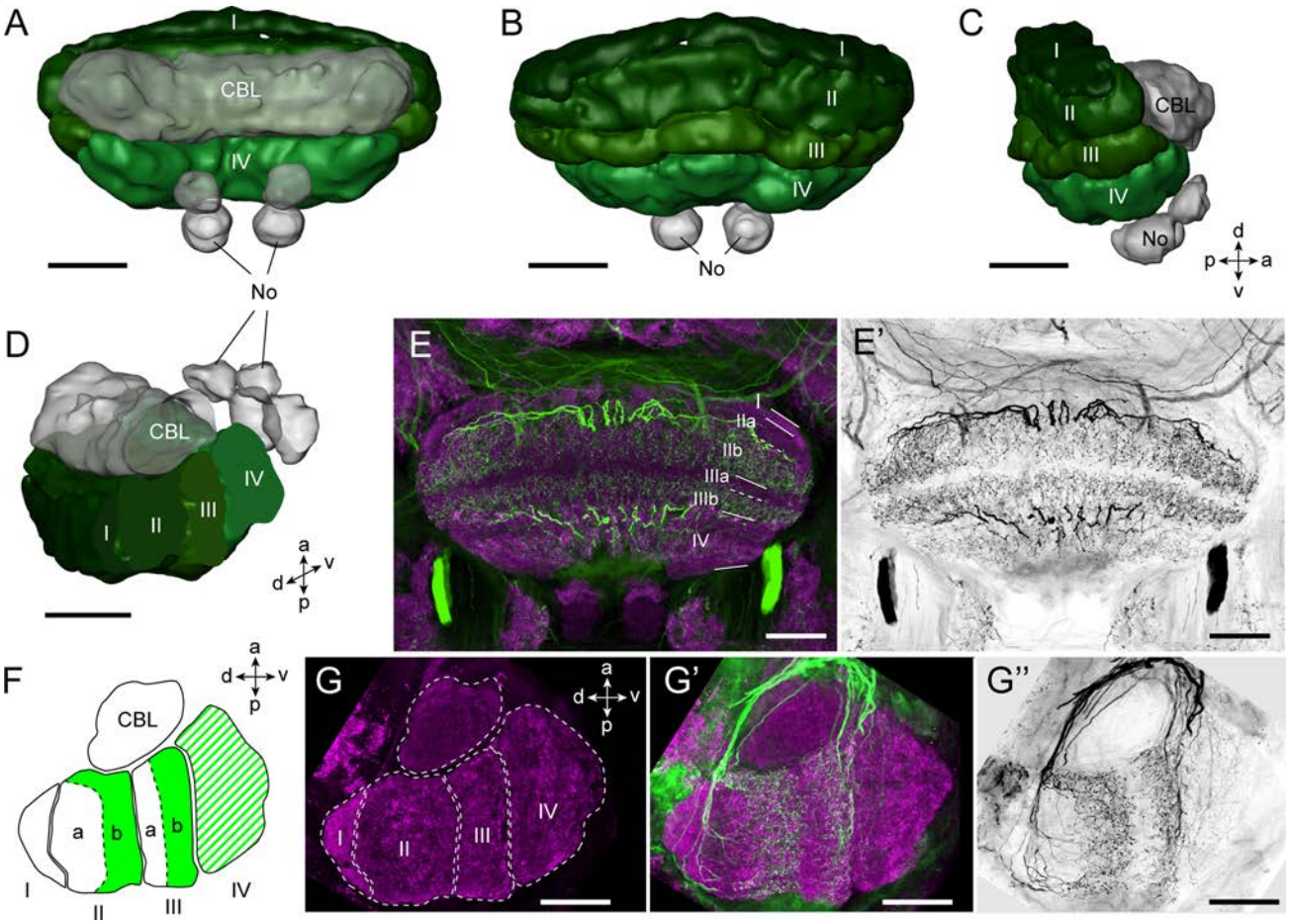


COLOR

Figure 6. Anatomical organization of the upper division of the central body. **A–D:** 3D reconstructions of the central body (together with the noduli) based on synapsin-ir. The upper division of the central body (CBU) is shown in green, while the remaining central-complex components are shown in gray. Four horizontal layers of the CBU could be distinguished (I–IV). A: anterior view; B: posterior view; C: lateral view; and D: oblique view cut along the sagittal plane to expose cross section of layers. **E:** Confocal images (maximal intensity projections; depth: 18 images; stepsize: 1 μm) of frontal vibratome sections of the CBU stained against serotonin (green in E, black in **E′**) and synapsin (magenta). Superposition of both stainings is shown in E, while only serotonin-ir (inverted, monochrome) is shown in E′. Serotonin-ir allowed refining the definition of layers in the CBU (sublayers indicated by a/b). **F:** Schematic representation of CBU layers based on synapsin-ir and serotonin-ir. Green color illustrates presence of serotonin-ir. Hatched green area indicates weak serotonin-ir. **G:** Confocal images of the CBU as in E, but cut in the sagittal plane. Note that the image of synapsin-ir in G contains only a subset of the optical sections (12 images) used for the maximal intensity projections in G′ and G″ (depth: 40 images; stepsize: 1 μm) for clarity. Scale bars = 50 μm.

to posterior (Fig. 7A–D). The smallest and anterior-most compartment appeared most distinct, as it was characterized by a much brighter appearance with anti-synapsin labeling.

The central body was analyzed in greatest detail. Although the CBL appeared largely homogeneous with anti-synapsin labeling (Fig. 5D–I), dye injections into the lateral triangle revealed a distinct stratification of the CBL generated by tangential neurons (Fig. 5J–K). At least four layers could be distinguished; two narrow sheet-like strata on the ventral side, a tubular layer in the center, and a fourth layer enclosing the central one on the dorsal side.

An even more complex subcompartmentation was observed in the CBU. Based on synapsin-ir alone, four layers could be distinguished, arranged in a linear stack from dorsal to ventral (Fig. 6A–D). The first one is a thin, brightly stained layer on the very dorsal edge of the CBU. It is followed by a second thick, more dimly stained layer, which merges into the third layer ventrally. Layers two and three could be separated clearly on the posterior portion of the CBU, but were less distinct on the anterior side. The fourth layer is located on the very ventral side of the CBU. Serotonin-ir confirmed the boundaries between all four layers and further allowed us to subdivide layers two and three, as serotonin-immunoreactivity terminals



ID: sureshkumard | Black Lining: [ON] | Time: 20:30 | Path: N:/3b2/CNE#/Vol00000/120021/APPFile/JW-CNE#120021

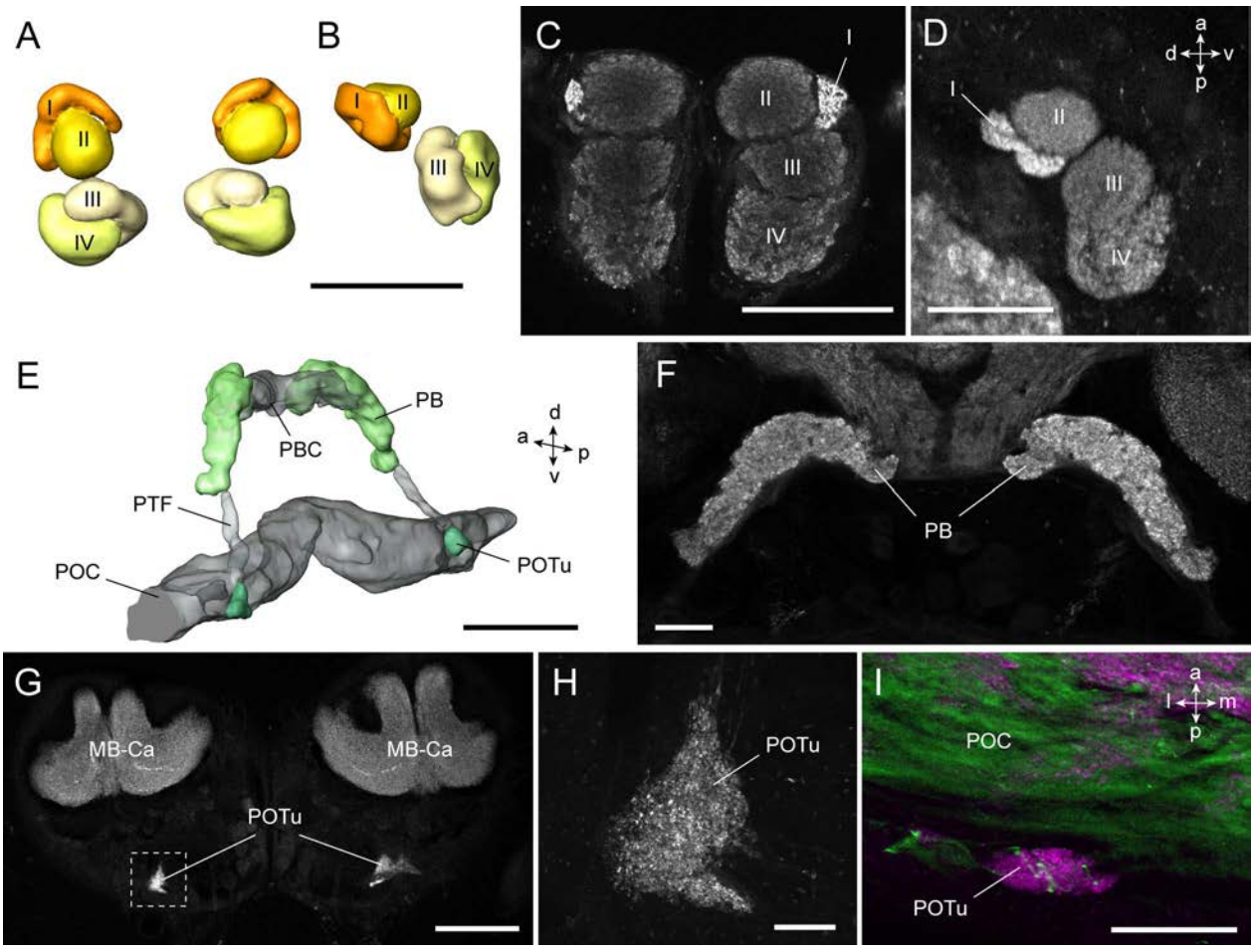


COLOR

**Figure 7.** Anatomical organization of the remaining neuropils of the central complex and posterior optic tubercle (POTu). **A,B:** 3D reconstruction of the noduli based on synapsin-ir, revealing the four compartments of each nodulus (A: anterior view; B: lateral view). **C,D:** Confocal images of anti-synapsin labeled vibratome sections showing the noduli with their compartmentation (layers I–IV). C: Horizontal section; D: sagittal. **E:** 3D reconstruction of the protocerebral bridge (PB) and its connection to the POTu, oblique view. Neuropils are shown in green, while fiber bundles are shown in gray. **F:** Superposition of two optical sections from adjacent frontal vibratome sections showing the PB. **G,H:** Confocal images (G: single optical section; H: maximal intensity projection; depth: 16 images; stepsize: 1 μm) of an anti-synapsin labeled, frontal section illustrating the location of the POTu with respect to the mushroom body calyces. The dashed square indicates location of the enlargement shown in H. Note the irregular shape of the POTu. **I:** Maximal intensity projection (depth: 17 images, stepsize 1 μm) of a horizontal section through the POTu stained against serotonin (green) and synapsin (magenta). The channel containing the serotonin-ir was deliberately overexposed to reveal faint background staining for visualization of the posterior optic commissure. The posterior surface of the brain lies directly posterior of the POTu. PTF, protocerebral bridge tubercle fascicle; PBC, protocerebral bridge commissure. Scale bars = 50 μm in C,D,F,I; 100 μm in E; 200 μm in G; 20 μm in H.

are only present in their ventral halves (Fig. 6E–G). Layer four is uniformly filled with dimly stained serotonin-immunoreactivity fibers. Overall, the six identified strata of the CBU create a coordinate system that allows localizing arborization trees of neurons with great precision within the boundaries of this structure (Fig. 6F). The clear columnar organization observed in the central body of some insects (e.g., crickets, wasps, [Schildberger, 1983; Strausfeld, 1999]) was not obvious in the monarch. All vertical columns of the central body appear to be completely fused.

Besides the LAL, another neuropil is closely associated with the central complex, namely, the posterior optic tubercle. This small neuropil has not been described as distinct neuropil in holometabolous insects before, but is well defined in locusts and cockroaches (Homberg et al., 1991). In the monarch it is located on the very posterior margin of the brain, between the posterior optic commissure and the surface of the brain (Fig. 7G–I). It is a flat, irregular-shaped structure and was identified by tracing projections of tangential neurons of the PB, which are known to innervate the posterior optic tubercle in locusts (Heinze and Homberg, 2007; Heinze and Reppert, 2011). It appears to be the largest of several synaptic neuropil inclusions embedded in the posterior optic commissure.



ID: sureshkumard | Black Lining: [ON] | Time: 20:30 | Path: N:/3b2/CNE#/Vol00000/120021/APPFile/JW-CNE#120021

## A monarch-specific visual neuropil?

Surprisingly, one of the brightest synapsin-immunoreactivity structures in the monarch brain was a region without any obvious resemblance in other insects. This neuropil is located within the optic stalk and stretches from the medial margin of the lobula to the lateral boundary of the mushroom body calyx at the posterior limit of the central brain (Fig. 8). It appeared as a multilobed, irregularly shaped region with very distinct boundaries, but without any obvious subcompartmentation. On its anterior side this structure is a thin, tube-like neuropil and gradually turns into a thick, bulbous structure toward its posterior end. Judging from background staining, fiber bundles appear to connect the structure with the lobula on its lateral end, while fibers emerging from the medial end of the structure lead partly into the direction of the mushroom body calyx. Due to the intense staining typical for optic glomeruli and its likely input from the lobula, we hypothesize that this neuropil is a conglomerate of optic glomeruli and termed it the optic glomerular complex.

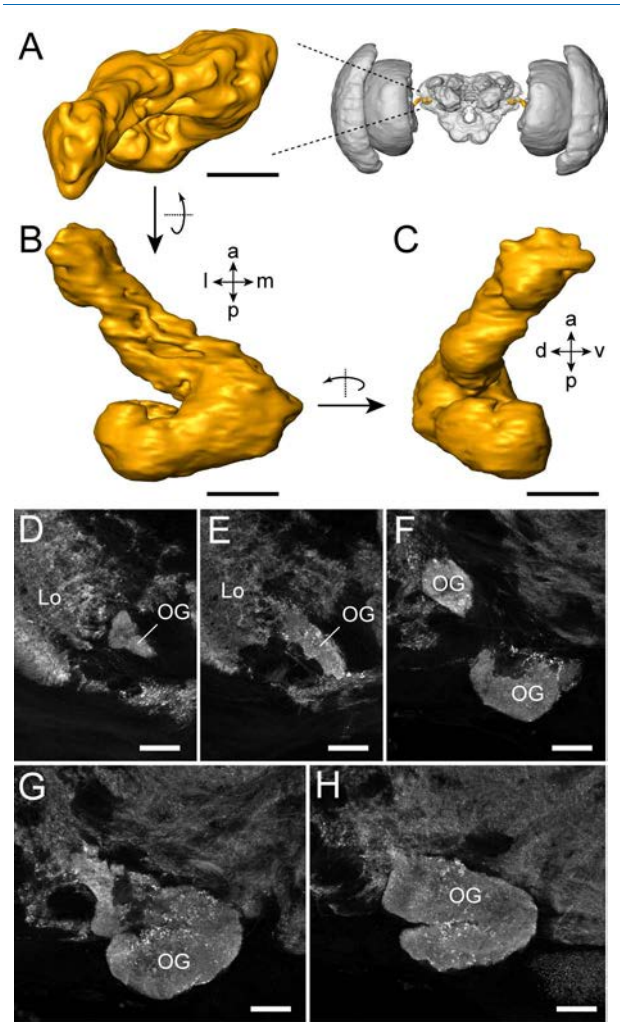


COLOR

**Figure 8.** Anatomical organization of the optic glomerular complex. **A–C:** 3D reconstruction of the optic glomerular complex (OG; right hemisphere), a newly identified monarch butterfly neuropil located between the lobula and the mushroom body calyx, embedded in the posterior lateral protocerebrum (location illustrated in A, together with a whole brain reconstruction in gray) (A: anterior view; B: ventral view; C: lateral view). **D–H:** Confocal images of horizontal vibratome sections stained against synapsin (maximal intensity projections; depth: 16–19 images; stepsize: 1 μm). Sections cover the right OG from ventral to dorsal (D–H). Scale bars = 50 μm.

## Olfactory system

Although monarch butterflies are mainly guided by skylight cues, i.e. visual information, during their migration, the neuroarchitecture of the olfactory system must also be considered for two reasons. First, it has been shown that circadian clocks located in the antennae are essential for time-compensated sun compass navigation in monarchs (Merlin et al., 2009). Thus, defining the anatomy of the antennal lobes and mushroom bodies will provide a frame of reference in which to characterize antennal projections and their potential links to the sun compass system in the central brain. The second reason is that olfactory cues have been proposed to play a role in the final segment of the monarch migration; that is, they might govern the monarch's ability to locate their specific overwintering sites, the rare oyamel fir groves (Reppert et al., 2010).

## Antennal lobes

The monarch antennal lobes are the largest neuropils of the central brain, occupying nearly 10% of its space. They are located on the anterior side of the brain and are clearly visible as spherical protrusions on either side of the oesophagus. The antennal nerves, originating from the antennal base at the apex of the monarch head, target the antennal lobes from dorsolaterally. After providing the olfactory receptor neurons to the AL, the antennal tracts run posterior-laterally alongside the ALs, and supply a large number of fibers to the antennomechanosensory and motor center (AMMC). Two major fascicles leave the posterior side of the AL, carrying olfactory information to higher brain centers: the large medial antennocerebral tract and the mediolateral antennocerebral tract, both sharing the same root on the posteromedial side of the AL. The lateral antennocerebral tract, prominent in numerous other insects, could not be easily distinguished in the monarch with the methods used.

As in most insects, the monarch antennal lobes are composed of a multitude of roundish subcompartments, called glomeruli, arranged spherically around a central fibrous neuropil region (Fig. 9). Somata are located in two characteristic clusters: the large lateral cell group,

characterized by intense GABA-immunoreactivity, presumably originating from GABA-ir local interneurons, and the much smaller medial cell group, which lacks GABA-ir (Fig. 9C). In both groups antennal lobe projection neurons could be found (unpubl. obs.).

The glomeruli generally possessed a center surround organization, consisting of a distal rind and an inner core. Although this was partly visible with anti-synapsin labeling, GABA- and serotonin-ir was confined to the core regions and thus revealed this structural organization

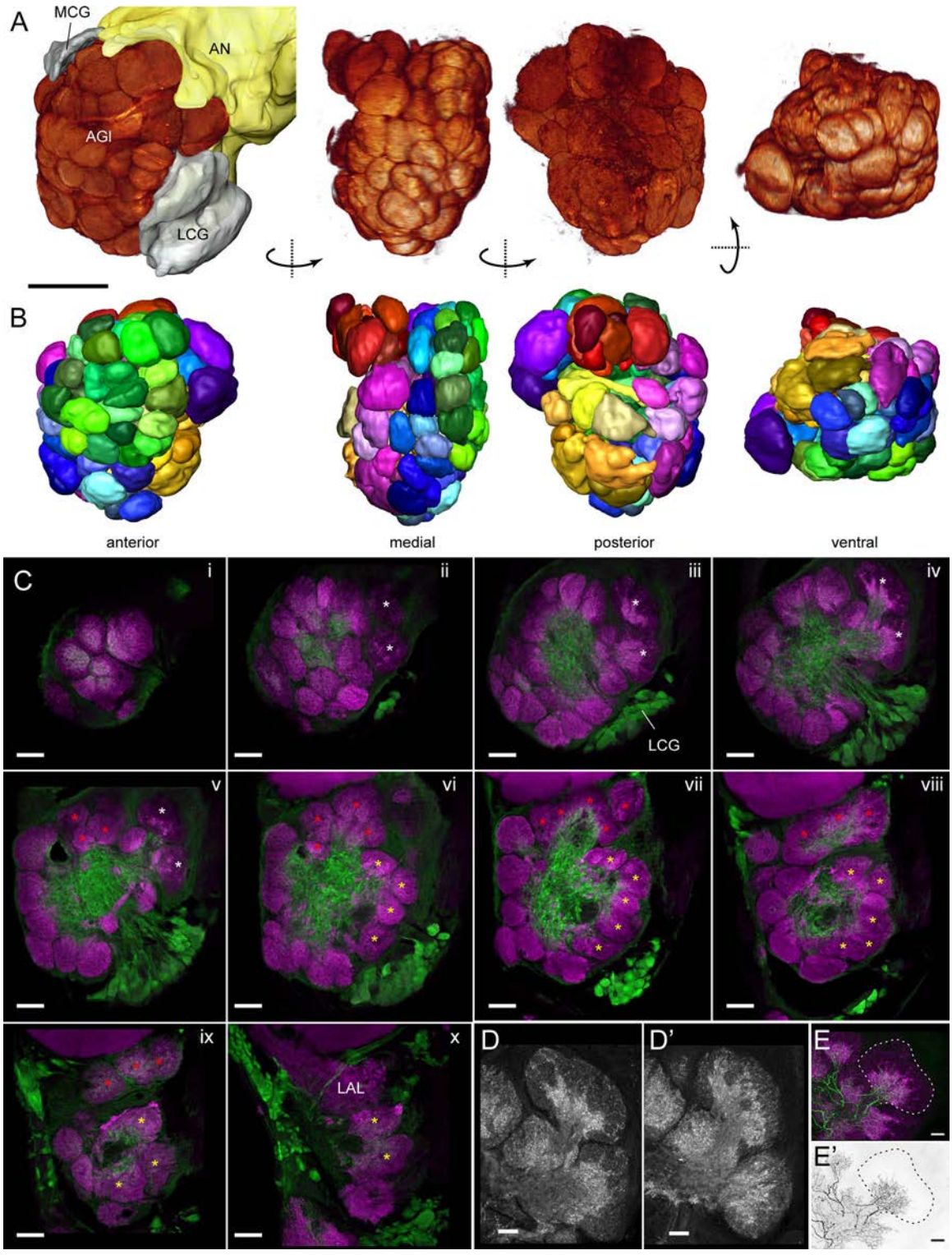


Figure 9

with great clarity (Fig. 9C–E). Glomeruli could be divided into four major groups based on their morphological features and location (Fig. 9B). The first and largest group was composed of 47 well-defined, typical glomeruli, which cover the complete anterior side of the AL, as well as much of its medial and ventral sides. Based on distance from the anterior limit of the AL, this group was further divided into an anterior layer, an intermediate layer, and a posterior layer (Fig. 9B). The second major set of glomeruli consists of at least 9–10 irregularly shaped glomeruli without very distinct boundaries, which often show elongated protrusions into the central neuropil (Fig. 9B,C). This group occupies the lateral (posterior of the lateral cell group) and posterior part of the AL (anterior of the LAL). The third group is a collection of ≈9–13 glomeruli that can be found at the dorsoposterior side of the AL, bordered by the mushroom body lobes (dorsally) and the LAL (posteriorly). Despite having a well-defined outer boundary, most of these glomeruli merge with one another near the central neuropil, making a clear separation of individual glomeruli difficult (Fig. 9B,C). The fourth group is composed of two very large glomeruli. They are located near the entry point of the antennal tract at the dorsolateral limit of the AL and have well-delineated boundaries. Despite being reminiscent of the sex-specific glomeruli in moths by shape, internal appearance, and location, these two glomeruli were indistinguishable between male and female monarchs (Fig. 9D).

## Mushroom bodies

The last remaining clearly defined neuropils of the monarch brain are the mushroom bodies, the major higher-order processing centers for olfactory information and for learning and memory in many insects (Strausfeld et al., 2009). In the monarch, as in most insects, the mushroom bodies are composed of the posteriorly located calyx, the anteriorly located lobes, and the pedunculus, which provides the connection from the calyx to the lobes (Fig. 10A). F10

The monarch butterfly calyx lies at the very posterior limit of the brain on either side of the midline, occupying roughly two-thirds of the width of the central brain within each hemisphere. The main calyx consists of two medially fused, cup-shaped single calyces, the lateral calyx and the medial calyx, both arranged roughly horizontally (Fig. 10A–F). Each of these structures are composed of three concentric neuropils, the inner zone, the outer zone, and the basal zone. The outer zone is a well-defined, doughnut-shaped neuropil at the outer, posterior rim of each calyx. It has a denser structure compared with the other two compartments and was thus easily identified. The inner zone is also toroid-shaped and occupies the space inside the outer zone. Although its posterior boundary is clearly defined, it partly merges with the basal zone in more anterior regions. The basal zone itself consists of a ring-like neuropil just anterior of the outer zone, and a posterior protrusion that is located between the lateral and the medial calyx, extending all the way to the posterior limit of the calyx (Fig. 10A–F). The posterior protrusion and the basal rings of the lateral and medial calyces are fused medially. In addition to these main structures, we observed a small neuropil area on the anterior side of the calyx, just ventral of the pedunculus. This unpaired region, the accessory calyx, protrudes slightly into the gap between the lateral and the medial calyx and sends one fiber-like, yet synapsin-immunoreactivity appendage into each outer zone. Its anterior boundary is not well defined and merges with the surrounding posterior lateral protocerebrum (Fig. 10R,S).

The pedunculus emerges from two roots in the center of the lateral and the medial calyx and fuses into a single, tube-like neuropil that runs vertically toward the anterior side of the brain. It exhibits a clear stratification consisting of at least five distinct layers (Fig.

Figure 9. Anatomical organization of the antennal lobes. **A:** Volume rendering of confocal image stacks obtained from wholemount preparations stained against synapsin. The antennal lobe was isolated by removing the surrounding parts of the image stack. The anterior view (left) contains, in addition to the antennal glomeruli (AGl), 3D reconstructions of the major cell groups of the antennal lobe (medial cell group, MCG; lateral cell group, LCG) and the proximal end of the antennal nerve (AN). **B:** 3D reconstructions of all individual antennal lobe glomeruli, viewed from different directions (indicated below images and correspond to those in A). The different colors correspond to identifiable groups of glomeruli: red tones, posterodorsal glomeruli; yellow tones, posteromedial glomeruli; violet, two large glomeruli likely corresponding to the macroglomerular complex of moths (macroglomeruli). The remaining glomeruli (green, blue, pink) comprise all ordinary, well-defined glomeruli (anterior layer, green; middle layer, blue; posterior layer, pink). **C:** Series of confocal images (frontal plane) stained against GABA (green) and synapsin (magenta) covering the whole antennal lobe from anterior (i) to posterior (x) at 30-μm intervals. GABA-ir reveals the location and size of the lateral cell group, as well as the outline of the central, aglomerular neuropil. Within the glomeruli, GABA-ir is restricted to their core. White asterisks in indicate the two macroglomeruli at the base of the antennal nerve; yellow asterisks indicate yellow glomeruli from B; red asterisks indicate red glomeruli from B. **D,D′:** Confocal images of the two macroglomeruli. Male and female preparations, respectively, were indistinguishable. **E,E′:** Confocal images (maximal intensity projections; depth: 17 images; stepsize: 1 μm) of frontal sections stained against serotonin (green in E, black in E′) and synapsin (magenta in E), illustrating the zonation of glomeruli (core, cortex). Scale bars = 50 μm in A–C; 20 μm in D,E.



ID: sureshkumard | Black Lining: [ON] | Time: 20:31 | Path: N:/3b2/CNE#/Vol00000/120021/APPFile/JW-CNE#120021

10M–P). These layers are arranged horizontally near the calyx and gradually twist medially further anterior. Before giving rise to the lobe system at the anterior limit of the pedunculus, the layers are arranged approximately vertically.

The mushroom body lobes in insects generally consist of the vertical lobe system and the medial lobe system, each being further subdivided into two or three individual lobes. In lepidopterans a third lobe system, the Y-tract with one or two associated loblets, is frequently observed

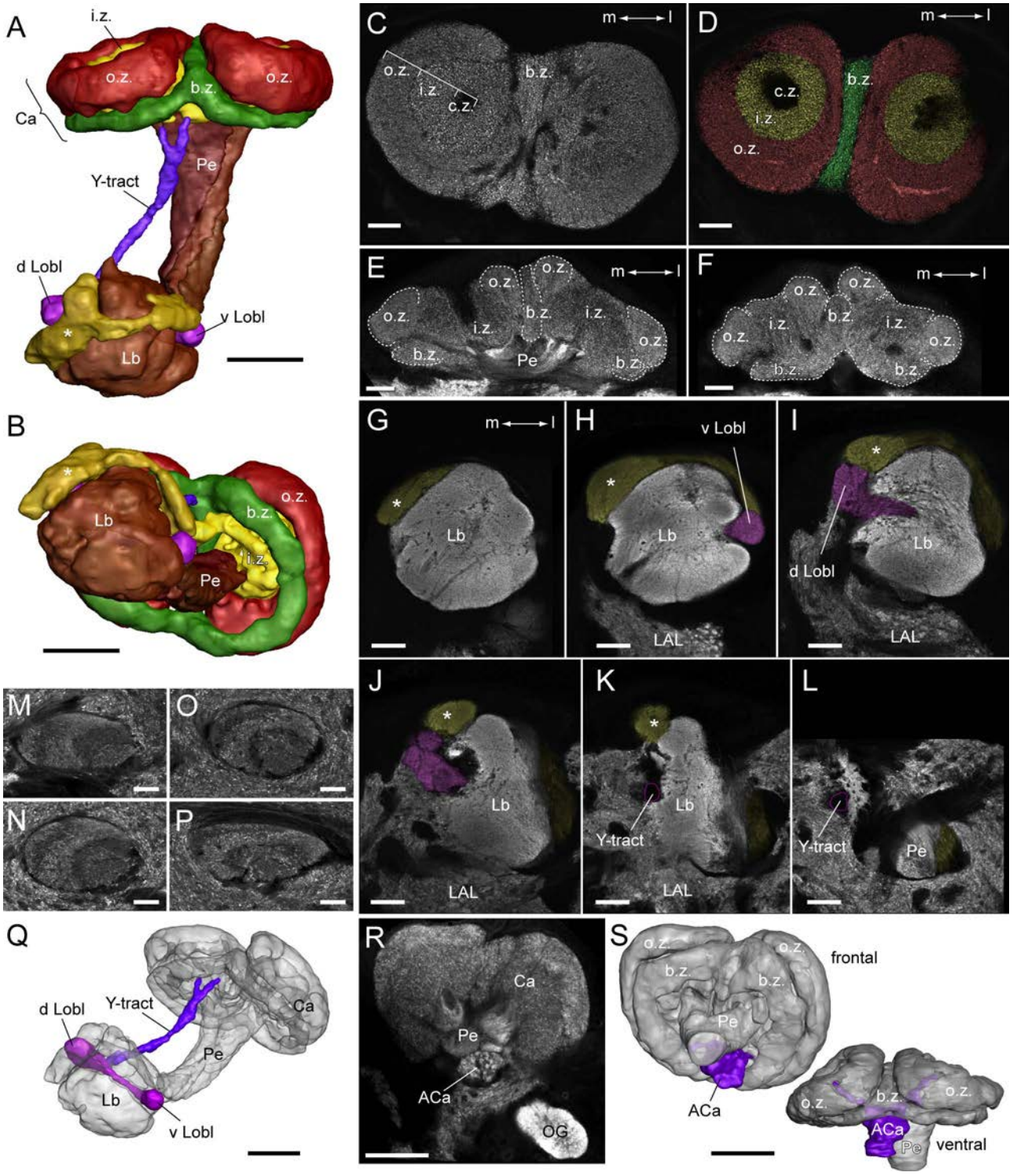


Figure 10

(Pearson, 1971; Sjöholm et al., 2005). In the monarch, the lobe system is highly compressed and appears as a smooth, homogeneous structure of roughly spherical shape (Fig. 10G–L). The vertical and medial lobe systems are fused and only one of their individual components could be reconstructed separately. Owing to its location on the dorsal side, this lobe is likely part of the vertical lobe system (Fig. 10A,B,G–L). The Y-tract with its associated dorsal and ventral loblets could be identified unambiguously (Fig. 10A,Q). The two loblets are located on the medial and lateral margins of the remaining lobes and are connected by a neuropil bridge that centrally intersects with the remaining lobes in an oblique direction. Emerging from the larger dorsal loblet, the Y-tract runs parallel to the pedunculus at the boundary of inferior and superior protocerebrum and is connected with the calyx at the intersection of the medial and lateral calyces.

## Unspecified neuropils in the central brain

Although we have described all major neuropils of the monarch brain, it is important to note that up to now we have covered only ≈30% of all of the synaptic neuropil of the central brain (Fig. 11A–C). The remaining regions occupy the space in between the well-defined neuropils and can be summarized by the term unspecified neuropils of the brain. These generally underdescribed regions are intricately connected with the optic lobes and the central body, receive a variety of sensory inputs, and are the origin of most descending neurons. Until detailed descriptions of neuronal projection patterns and developmental data become available for the monarch brain, the boundaries within the unspecified neuropils remain largely preliminary. However, they provide a helpful framework for locating and discussing future and ongoing anatomical results. Whenever identical names were applied to a monarch neuropil compared with potential counterparts in other species, the implied homology is based on the relative location of the neuropil with respect to surrounding structures. It does not verify that the regions are truly homologous or that the chosen boundaries are indeed fully comparable. Hence, it is entirely possible that with more comprehensive data, neuropil boundaries will move slightly, resulting in reallocation of subcompartments of one neuropil to another.

In broad terms, we divided the unspecified neuropils of the monarch brain into five major groups: the superior neuropils, the lateral neuropils, the inferior neuropils, the ventromedial neuropils, and the suboesophageal neuropils (Fig. 11A–C,E). Other than the defined neuropils, four easily identifiable landmarks were used to draw reproducible boundaries—the great commissure, the pedunculi of the mushroom bodies, the Y-tracts of the mushroom bodies, and the lateral fiber fascicle connecting the central body with the PB (containing the w-bundle) (Fig. 11D).

### *Superior neuropils*

These regions are located at the dorsal boundary of the brain and consist of the superior medial protocerebrum (SMP, dorsal and ventral shell), the superior lateral protocerebrum (SLP), and the lateral horn (Fig. 11A–C,E). They are bordered by the inferior neuropils on the ventromedial side and by the lateral neuropils on the ventrolateral side. All compartments, except the one directly bordering the midline, showed a smooth, homogeneous synapsin-ir, different from all other brain regions (Fig. 11A).

In detail, the ventral shell of the SMP is adjacent to the midline, lines the dorsal wall of the central-complex cavity, and, further posterior, is bordered by the midline

**Figure 10.** Anatomical organization of the mushroom bodies. **A,B:** 3D reconstruction of the mushroom body based on synapsin-ir in a wholemount preparation. Shown are all identifiable subregions; in the calyx (Ca) these are the inner zone (i.z.), the outer zone (o.z.), and the basal zone (b.z.); the Y-tract and its associated dorsal loblet (d Lobl) and ventral loblet (v Lobl) could also be identified. In the main lobe system, one region could be separated (indicated by the asterisk) and is likely part of the vertical lobe. In the pedunculus (Pe), three layers were reconstructed to illustrate the twist of the structure. A: dorsal view (posterior is up, medial is left); B: anterior view (dorsal direction is up). **C,D:** Confocal images of frontal vibratome sections stained against synapsin, illustrating the fine structure of the calyx. D (posterior section) was superimposed by colors corresponding to A,B. **E,F:** Confocal images of horizontal sections stained against synapsin. Zonal boundaries are indicated by dashed lines. E: A section through the center of the calyx, while F lies further dorsal. **G–L:** Confocal images of frontal sections through the mushroom body lobe systems, stained against synapsin. The image series covers the lobes from anterior to posterior (G–L) and highlights their fused nature. Only the lobes associated with the Y-tract (superimposed in pink) and one component of the main lobe system (likely part of the vertical lobe, superimposed in yellow and marked by asterisk) could be identified. **M–P:** Confocal images of cross-sections (frontal) of the pedunculus (M–P: anterior to posterior) stained against synapsin. At least five different layers can be identified in the pedunculus, twisting from vertical orientation (M) to near horizontal orientation (P). **Q:** 3D reconstruction (oblique view) highlighting the Y-tract with its associated loblets (rest of the mushroom body in gray). **R:** Confocal image of anti-synapsin-labeled wholemount preparation (frontal optical section), illustrating the location and appearance of the accessory calyx (ACa). **S:** 3D reconstruction of the calyx (gray) highlighting the ACa (violet). Viewing angles are indicated; posterior direction is up in ventral view. Note that the anterior boundary of the ACa is not well defined and was arbitrarily cut off. The posterior, fibrous appendages (ventral view) are also visible as bright staining within the calyx outer zone in D (right image). Scale bars = 100 μm in A,B,Q–S; 50 μm in C–L; 20 μm in M–P.



ID: sureshkumard | Black Lining: [ON] | Time: 20:31 | Path: N:/3b2/CNE#/Vol00000/120021/APPFile/JW-CNE#120021

spanning posterior medial protocerebrum (PMP). Its posterior extent defines the posterior brain surface in that region, while the anterior end is contiguous with the anterior inferior protocerebrum (AIP). Their border was arbitrarily defined at the level of the posterior limit of the CBL (roughly the level of the giant commissure). Laterally, the ventral shell of the SMP borders the superoposterior inferior protocerebrum (SPIP) and the dorsal shell of the SMP. The distinguishing feature of the ventral shell of the SMP is its brighter synapsin-ir, which appears coarser compared with the remaining superior neuropils. The dorsal shell of the SMP encloses the ventral shell dorsally and extends further laterally. It is contiguous with the SLP, which begins (arbitrarily) at the level of the pedunculus; that is, all superior neuropil located medially of the pedunculus is SMP, while all superior neuropil located laterally of this line is SLP. Ventrally, the dorsal shell of the SMP is bordered by the SPIP. The Y-tract of the

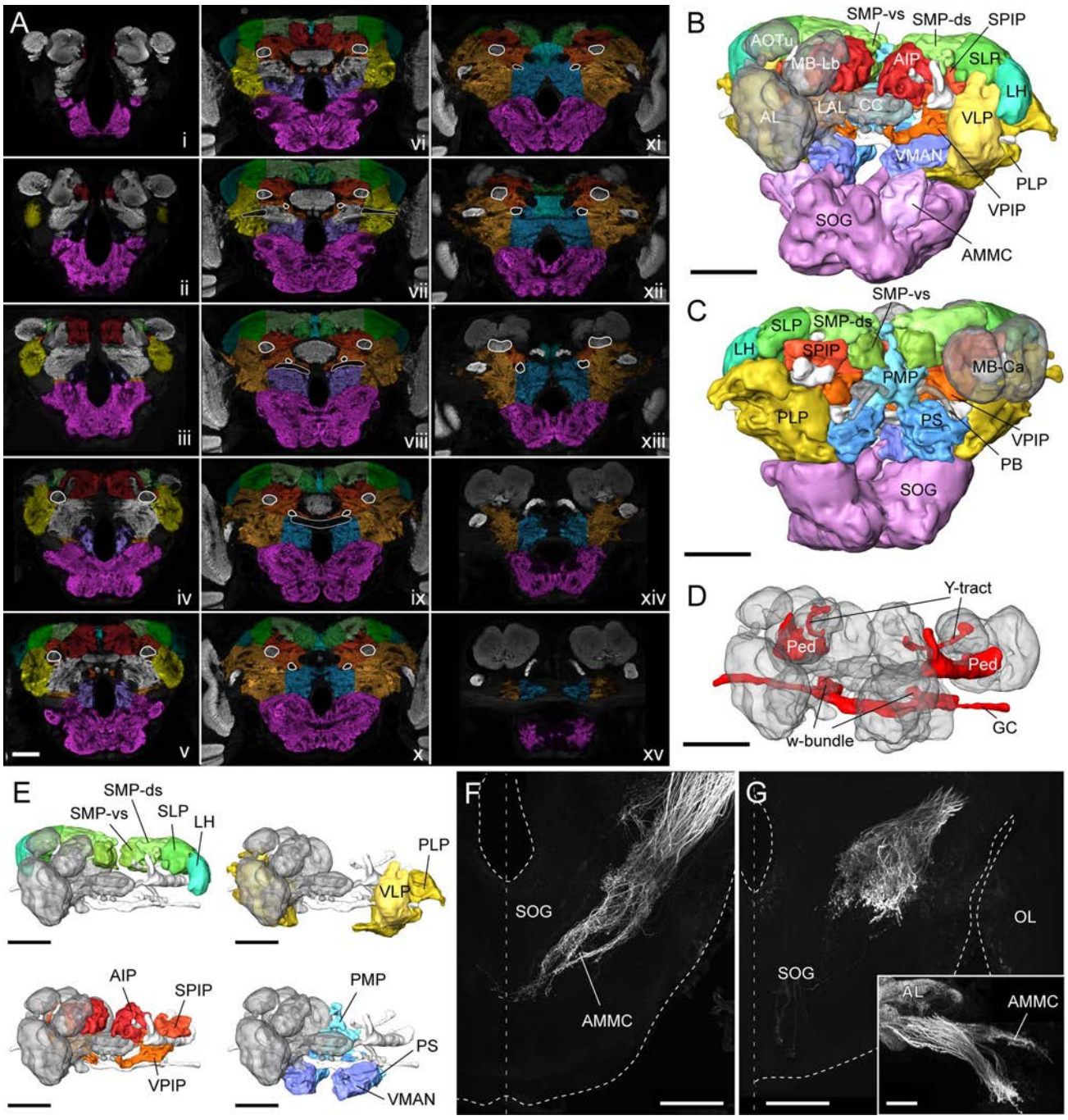


Figure 11

mushroom body runs approximately along this boundary, before it bends ventrally and becomes enclosed by the AIP. In its anterior extreme the dorsal shell of the SMP comprises the small neuropil between the AOTu and the mushroom body lobes. The SLP begins medially at the level of the pedunculus, while ventromedially it borders the SPIP. Ventrolaterally its border with the lateral protocerebrum was difficult to identify and was defined in an approximately diagonal line from the pedunculus to the dorsolateral corner of the brain. Finally, the AOTu defined the limits of the SLP on the anterior side. The lateral horn was included as the lateral-most compartment of the superior neuropils due to the lack of a clear boundary and its similar appearance with anti-synapsin labeling. Its identity and location were confirmed by dye filling of antennal lobe projection neurons ($n = 5$, not shown).

### *Lateral neuropils*

These regions are roughly positioned between the LAL and the optic lobe and consist of the ventrolateral protocerebrum (VLP) and the posterior lateral protocerebrum (PLP; Fig. 11B,C,E). The two neuropils are separated by the great commissure and bordered dorsally by the superior neuropils, while the pedunculus, the LAL, the ventromedial, and the inferior neuropils are located medially. Except for the anterior-most part of the VLP these neuropils are characterized by foci of dense synapsin-ir, reminiscent of optic glomeruli of *Drosophila* (Otsuna and Ito, 2006). Accordingly, the optic glomerular complex is embedded within this region (Fig. 11A). The VLP forms the anterior surface of the central brain neuropil, lateral of the LAL and ventral of the AOTu. Its medial boundaries are defined by the LAL and the pedunculus, while dorsally the SLP, lateral horn, and AOTu define its limits. The PLP covers all of the lateral brain ventral of the superior neuropils and dorsal of the SOG. Its medial limit does coincide with the disappearance of synaptic foci. Despite this, the medial boundary is not clearly delineated and had to be arbitrarily chosen in some areas. The boundary to the superior neuropils follows a diagonal line from the pedunculus to the dorsolateral edge of the brain. The boundary to the inferior protocerebrum follows the line connecting the pedunculus with the w-bundle. Further ventral, its boundary with the posterior slope (PS) follows a straight dorsoventral line from the w-bundle toward the SOG. Additionally, the narrow stretch of neuropil between the LAL and the SOG was also allocated to the PLP, as it seemed most contiguous with this region.

### *Inferior neuropils*

The three inferior neuropils fill the space between the cavity that contains the central body and the components of the mushroom body (Fig. 11A–C,E). It is composed of an anterior, medial region directly adjacent to the mushroom body lobes (AIP), and a more posterior region bordered by the pedunculus. The latter region could be divided into a ventral and a superior part (ventroposterior inferior and superoposterior protocerebrum; VPIP, SPIP) at the level of the pedunculus, and stretches all the way to the posterior boundary of the brain. Ventrally the inferior neuropils are limited by the LAL, the great commissure, and the w-bundle, whereas the dorsal boundary is formed by the superior neuropils (Fig. 11A). In detail, the AIP spans the space between the mushroom body lobes

**Figure 11.** Anatomical organization of unspecified neuropils in the monarch brain. **A:** Confocal image series (frontal plane, synapsin-ir) covering the central brain from anterior (i) to posterior (xv) at 30-μm intervals. Colored overlays semischematically show the compartments of the unspecified neuropils. All areas remaining gray are well-defined, classic neuropils (compare Figs. 2–10). The colors correspond to the reconstructions shown in B, C, and E. White outlines highlight structures used as orientation cues in the brain (pedunculus, giant commissure, and the w-bundles). Labels have not been added to preserve clarity; for identity of the different regions refer to B–E. **B,C:** 3D reconstruction of the central brain based on synapsin-ir in a wholemount preparation. Well-defined neuropils are shown in transparent gray (left side neuropils removed for clarity). B: oblique anterior view; C: oblique posterior. **D:** 3D reconstruction of the orientation cues (red) used to define the boundaries of the unspecified neuropils together with the classic neuropils (gray). **E:** 3D reconstructions of the four groups of neuropils comprising the supraoesophageal part of the unspecified neuropils (reconstructions are details from B in identical orientation). Superior neuropils are shown in shades of green, lateral neuropils in shades of yellow, inferior neuropils in shades of red, and ventromedial neuropils in shades of blue. **F,G:** Confocal images (maximal intensity projections; depth: 70 images, stepsize: 2 μm (F); depth: 87 images, stepsize: 2 μm (G)) of neurobiotin backfills of the antennal nerve. Antennal projections to the suboesophageal ganglion (SOG) constitute the antennomechanosensory and motor center (AMMC) and can be divided into two distinct domains: an anterior, midline crossing domain (F), and a posterior, lateral domain (G). The inset in G shows a lateral maximal intensity projection (depth: 220 images, stepsize: 2 μm) of one preparation revealing the relative location of both projection areas and the antennal lobe. SMP-ds, dorsal shell of the superior medial protocerebrum; SMP-vs, ventral shell of the superior medial protocerebrum; SLP, superior lateral protocerebrum; LH, lateral horn; VLP, ventrolateral protocerebrum; PLP, posterior lateral protocerebrum; AIP, anterior inferior protocerebrum; SPIP, superoposterior inferior protocerebrum; VPIP, ventroposterior inferior protocerebrum; PMP, posterior medial protocerebrum; PS, posterior slope; VMAN, ventromedial anterior neuropil; GC giant commissure. Scale bars = 200 μm in A–E; 100 μm in F,G.

and the midline, dorsal of the LAL. It lines the posterior side of the mushroom body lobe system and extends posteriorly to the level of the posterior limit of the CBL. There it is contiguous with the ventral shell of the SMP, with which it shares its bright, rather coarse appearance in anti-synapsin-labeled preparations. The lateral boundary with the SPIP is based on a difference in tissue appearance and the presence of several fiber bundles, but generally it is not well defined. On its ventral side, the AIP is completely contiguous with the LAL, whose end has been defined at the level of the dorsal limit of the isthmus tract. Further medial, this neuropil lines the dorsomedial part of the central-body cavity. The SPIP wraps the dorsomedial side of the pedunculus and fills the space between the pedunculus and the central body. On its ventral side lies the VPIP, while on the dorsal side it is bordered by the superior protocerebrum. It can be distinguished from the latter by its different appearance with anti-synapsin labeling and the location of the Y-tract of the mushroom body along that border. The ventral limit was defined at the level of the pedunculus (horizontal plane). As it does not completely engulf the pedunculus, it borders the lateral protocerebrum on the pedunculus' distal side. The VPIP lies adjacent to the SPIP and ventrally extends this structure, filling the space between the central body, pedunculus, and LAL. Its ventral border (anteriorly) was defined at the level of the giant commissure, where it partly fuses with the ventromedial anterior neuropil (VMAN). Further posterior, the w-bundle provides a landmark separating the VPIP from the PS. On the lateral side, it borders the PLP and is separated from this neuropil along a line connecting the w-bundle and the pedunculus.

### *Ventromedial neuropils*

These regions consist of three parts. On the posterior side, these neuropils line the surface of the brain with the ventrally located PS and the more dorsal posterior medial protocerebrum (PMP; Fig. 11C). The latter covers the medial region in the posterior brain, between the central body and the PB. It is completely fused across the midline and borders the PS (ventrally), the inferior neuropils (laterally), and the ventral shell of the SMP (dorsolaterally). Irregularly shaped neuropil fragments stretching anteriorly along the midline have also been assigned to the PMP, as they seemed to originate from that structure. The PS ends ventrally on the level of the posterior optic commissure. Some irregular patches of synaptic neuropil extend into the commissure, leading to a frayed appearance of the posterior neuropil surface. Anteriorly, the limit of the PS was defined at the level of the giant commissure, in tune with other neuropils. The PS possesses an extensive boundary with the PLP, which largely correlates with the presence or absence of dense synaptic foci that are a characteristic feature of the PLP. In principle, this boundary follows a straight dorsoventral line ventral of the w-bundle. The w-bundle also marks the dorsal boundary of the PS with the VPIP. Anterior of the PS the VMAN was found (Fig. 11B,E). It covers the space between the LAL and the PS (boundary at the level of the giant commissure), as well as the neuropils medially of the LAL. The latter areas are anterior neuropil protrusions interspersed by fibrous regions, leading to a fragmented appearance. Several of these protrusions are contiguous with the LAL neuropil. Dorsally, the VMAN ends at the level of the giant commissure, where it merges with the VPIP. All ventromedial neuropils are bordered ventrally by the SOG, roughly at the level of the posterior optic commissure.

### *Suboesophagea neuropils*

The final mass of neuropils was found below the oesophagus and was included in the SOG. Except for the AMMC, no boundaries were drawn within this structure because of the lack of clear landmarks (Fig. 11A–C). Likely, further subdivision will become apparent in the regions occupying the space between the AMMC, the oesophagus, and the anterior surface of the brain with detailed studies of neuronal projection patterns. In wholemount preparations, the SOG often showed brighter synapsin-ir compared with the remaining brain, outlining its proposed boundary. This boundary roughly coincides with the vertical level of the posterior optic commissure. The AMMC is located ventroposteriorly of the ALs and extends into the SOG (Fig. 11B,F). Despite possessing a coarser, almost glomerular, slightly blurry appearance compared with its surroundings in anti-synapsin labeled wholemount preparations, the boundaries of the AMMC were not clearly delineated. Therefore, backfills of the antennal nerve were needed to reveal its outline (Fig. 11F,G). Based on 25 individual preparations from migratory and nonmigratory animals, the AMMC could be divided into two regions, an anterior area that stretches ventromedially away from the AL, and a smaller, distinct area that is located further posterior near the posterior margin of the brain (Fig 11F,G). The anterior AMMC reaches as far as, and in fact slightly across, the midline of the SOG. The thin terminals of the antennal sensory neurons are arranged in a loose meshwork, interspersed with regularly spaced foci of increased density (Fig. 11F). The posterior AMMC is much more uniformly organized, and the terminals are heavily beaded (Fig. 11G). Its partially distinct appearance in anti-synapsin labeled wholemount preparations allowed preliminary 3D reconstruction of the AMMC. However, this did not include the posterior component identified through the dye injections (Fig. 11G), leaving it for future experiments to map

antennal projections into a common frame of reference and thus defining the AMMC more comprehensively.

## DISCUSSION

In this study we used 3D reconstructions based on synapsin-ir in wholemount preparations to provide a comprehensive atlas of all neuropil areas of the monarch butterfly brain. The fine structure of these regions was further analyzed with the aid of brain sections stained against synapsin, serotonin, and GABA. Using contemporary methods, the current work builds on a historical study (Nordlander and Edwards, 1968) more than four decades ago, which, up to now, was the only attempt to describe the detailed structure of the monarch brain. Overall, our monarch brain atlas provides a comprehensive frame of reference for studying arborization patterns of single neurons, mapping the expression patterns of neurochemical substances, and charting the expression profiles of genes (by in situ hybridization). Additionally, our anatomical data can guide electrophysiological recordings to appropriate target areas.

### Broad outline of the monarch brain in relation to other insects

The brain of the monarch butterfly contains, as expected, all major components of a typical insect brain. Like many other holometabolous insects, but unlike locusts and cockroaches, the SOG is merged with the SPG to form the brain. This, as well as the combination of other gross features of the brain, in particular the presence of a lobula plate, the orientation of the mushroom bodies and the central complex, the lack of well-developed ocelli (Dickens and Eaton, 1973), and the large optic lobes and antennal lobes, are characteristic of the lepidopteran nature of the monarch butterfly brain.

For primary sensory areas, as well as for higher processing centers like central complex and mushroom bodies, it has been shown that the size of insect brain neuropils is directly related to their relative importance for the species (Gronenberg and Hölldobler, 1999; el Jundi et al., 2009; Wei et al., 2010). In this context, the large optic lobes are consistent with the diurnal, visually guided behavior of the monarch butterfly. Compared with other well-described insect brains, including moths, bees, flies, locusts, cockroaches, and beetles, the monarch butterfly possesses the largest optic lobes with respect to the remaining major neuropils (comparing only commonly reconstructed neuropils: medulla, lobula-complex, mushroom body, central body, antennal lobe) (el Jundi et al., 2009; Dreyer et al., 2010; Wei et al., 2010). To no great surprise, most anatomical similarities were found between the brains of the monarch and *Manduca*, consistent with the close evolutionary link between moths and butterflies.

The brain of *Manduca* has been reconstructed in a very similar way to what we have done for the monarch brain, allowing a more detailed interspecies comparison (el Jundi et al., 2009). The relative enlargement of the monarch optic lobe appears to be exclusively attributable to an increase in medulla volume (≈44% of total brain volume in monarchs vs. 28% in *Manduca*; while the remaining optic lobe occupied ≈30% of brain volume in monarchs vs. 31% in *Manduca*). When comparing neuropil volumes with respect to the size of the central brain, *Manduca* possesses ≥50% enlarged ALs, whereas all other neuropils (central complex, AOTu, mushroom body) were substantially larger in the monarch (more than twice as big in the case of the AOTu). The unspecified neuropils (including the LAL and optic glomerular complex) were identical in size. All of these differences are larger than the variability found for the *Manduca* neuropil volumes (standard deviations [SDs] between 6% and 20% for the neuropils included in the comparison; el Jundi et al., 2009). Considering that the variability in all other standardized insect brains occurs within comparable ranges and the finding that the variability within the monarch compass neuropils is similar between individual animals (SD 6–19%; $n = 10$; unpubl. data), the observed differences in gross neuropil ratios between the monarch and *Manduca* are unlikely due to sampling bias or chance. Furthermore, the described differences are consistent with a more visually guided behavior in monarchs (which are day-active and use vision for conspecific recognition) and a more olfactory guided behavior in *Manduca* (which are night-active and use pheromones for conspecific mate recognition).

### Interspecies comparison of the visual system emphasizing sun compass neuropils

A main reason for studying the anatomy of the monarch butterfly brain is to examine the structural basis of the monarch's ability to perform time-compensated sun compass navigation during the migratory generation. The question thus arises as to how similar the neuropils implicated in sun compass navigation in the monarch are to their counterparts in the desert locust, the only other long-distance migratory species that has been studied in detail (Homberg, 2004; Homberg et al., 2011).

The neurons likely involved in sun compass navigation can be identified by their ability to respond to plane polarized light, a response characteristic present only in very few neurons of the brain. Examples of polarization-sensitive (POL) neurons can be found in the monarch and the locust, and recent data suggest that they share a highly conserved morphology (Heinze and Reppert, 2011). The locust POL pathway involves the dorsal rim area (DRA) of



ID: sureshkumard | Black Lining: [ON] | Time: 20:31 | Path: N:/3b2/CNE#/Vol00000/120021/APPFile/JW-CNE#120021

the optic lobe, the medulla, the lobula, the AOTu, the LAL (including the lateral triangle), the central complex, and the posterior optic tubercle. What follows is a comparison of these locust brain regions to their monarch counterparts.

### *Optic lobe*

The locust POL-pathway (reviewed in Homberg et al., 2011) originates in the DRA of the compound eye, which is the eye region designated for detecting linearly polarized light in most insect species (Labhart and Meyer, 1999). From the DRA, photoreceptor axons project to specialized dorsal rim regions of the lamina and medulla. The DRA of the monarch eye is narrow and elongated, originates at the eye's apex, and stretches anteriorly (Stalleicken et al., 2006; Labhart et al., 2009). Photoreceptors of the DRA have been shown to project to the medulla (Sauman et al., 2005), which is consistent with the finding that monarch DRA photoreceptors are monochromatic for UV opsin. It remains unclear, however, whether the long, elongated neuropil area just anterior of the medulla (Fig. 2J–N) is merely an appendix of the accessory medulla or might play a role in polarized-light processing, owing to its exposed location similar to the dorsal rim medulla in the locust (Homberg and Paech, 2001). No region in the vicinity of the lamina was found in the monarch that resembled the dorsal rim lamina of the locust.

As in all insects, the monarch medulla had a highly stratified appearance. Although the number of 10 layers is identical in monarchs, locusts (Wendt and Homberg, 1992), and *Drosophila* (Fischbach and Dittrich, 1989), it is unlikely that the individual strata are indeed homologs, as in all cases different methods have been used to define them. Furthermore, it is different from the eight layers defined in the butterfly *Pieris brassicae* (Strausfeld and Blest, 1970). The most reliable and functionally meaningful definition of medulla layers is based on the systematic studies of Golgi impregnations of single neurons in flies (Strausfeld, 1970; Fischbach and Dittrich, 1989) and *Pieris* (Strausfeld and Blest, 1970). However, the definition of eight layers in blow flies (*Calliphora* species; Strausfeld, 1970) compared with 10 layers in *Drosophila* (Fischbach and Dittrich, 1989) using identical methods highlights that layers differ even in closely related species, or that different criteria were used for layer definition, making meaningful comparisons based on layers alone difficult. Nevertheless, these studies illustrate beautifully that cellular identities are widely conserved between species, and that conclusions about functional neuropil organization should be based on single-neuron data. Until such data become available for the monarch medulla, the stratification visible with the commonly used anti-synapsin labeling appears to be a valuable orientation aid for comparing neurons between individual monarch preparations.

The lobula and lobula plate of the monarch optic lobe has little resemblance with the lobula complex of the locust, which consists of four separate subunits with no lobula plate (Kurylas et al., 2008). Thus, there is no evidence that any part of the monarch lobula is the counterpart of the anterior lobula involved in the locust POL pathway. The structure of the monarch lobula clearly shares all major features with that of other moth species and flies (Strausfeld, 1976; Fischbach and Dittrich, 1989; Kvello et al., 2009; el Jundi et al., 2009).

### *Anterior optic tubercle*

In locusts, and also in bumblebees, line tangential neurons from the medulla provide the input to the AOTu, the next stage of the POL-pathway (Homberg et al., 2003; Pfeiffer and Kinoshita, 2012). The two subunits found in the locust (the upper and lower unit; Homberg et al., 2003) have also been reported in the bumblebee (Pfeiffer and Kinoshita, 2012), while three compartments were shown in the honeybee (Mota et al., 2011). Of the four compartments in the monarch, three (the upper unit, the lower unit, and the nodular unit) are also found in *Manduca*, while the strap region of the monarch AOTu seems to be unique (el Jundi et al., 2009; Huetteroth et al., 2010). Comparing AOTu anatomy across these species, a basic layout consisting of two subunits, a large upper unit (major unit in honeybees) and a small lower unit (ventrolateral unit in honeybees), appears common. A species-specific addition was found in the honeybee (lateral unit) and the monarch (strap), while lepidopterans possess a shared third unit (nodular unit). Preliminary data shows that monarch POL neurons receive input from one or several of the small units (Heinze and Reppert, 2011), suggesting their homology to the lower unit of the locust. Supporting this finding, neurons resembling locust POL-neurons have been reported in the lower unit of the bumblebee AOTu (Pfeiffer and Kinoshita, 2012), while visual responses originating in the main retina have been shown in the upper unit (major unit) of honeybees (Mota et al., 2011) and locusts (Pfeiffer et al., 2005). Overall, these data suggest a role of the insect AOTu in relaying functionally segregated visual pathways, one of which carries skylight information used for navigation.

### *Lateral accessory lobes*

POL neurons of the lower division of the locust AOTu project to two specialized regions in the LAL, the lateral triangle and the medial olive. From there, tangential neurons of the CBL provide input to the central complex. Homology of the lateral triangle between monarchs and locusts was clearly shown by GABA-ir. Additionally,

tangential neurons of the CBL possess input arborizations in this region in both species (Müller et al., 1997; Heinze and Reppert, 2011). Because of the lack of any nearby, strongly GABA-immunoreactivity neuropil connected to the CBL, the lateral triangle of the monarch likely resembles the combined lateral triangle and medial olive of the locust. This is consistent with data from *Drosophila* (Hanesch et al., 1989) and *Manduca* (Homberg et al., 1987), both of which also contain only one GABA-immunoreactivity neuropil in this area of the brain.

The remaining LAL consists of two major parts in the monarch, locust (Heinze and Homberg, 2008), and the silkworm *Bombyx mori* (Iwano et al., 2010): the dorsal and ventral LALs (dorsal/ventral shells in the locust). The whole area is rotated around the horizontal axis in the locust; hence the dorsal shell lies mostly anterior of the ventral shell. In contrast, both compartments reach the anterior limit of the LAL in the monarch and *Bombyx*. While the dorsal LAL is bordered by the medial lobes of the mushroom body and the antennal lobes, the ventral lobes extensively merge with the unspecified protocerebrum, so that they are much less distinct in their outline. In locusts, monarchs, and numerous other insects (Dacks et al., 2006) the ventral LALs are innervated by commissural serotonin-immunoreactivity neurons connecting both ventral LALs, while the dorsal LALs receive fibers from the CBU, suggesting that the two major LAL-subunits are indeed homologous between the two species (Homberg, 1991). The additional small anterior loblet of the monarch LAL had no apparent counterpart in the locust LAL. The remarkable microglomerular appearance of this structure, as well as the less pronounced but still distinct microglomeruli of the dorsal LAL, may be unique to the monarch, as they have no resemblance in any other species examined to date.

### *Central complex*

The central complex is the major integration site of the locust POL-pathway (Homberg et al., 2011). The monarch central complex contains all four components of a typical insect central complex (CBL, CBU, PB, and noduli). Compared with the locust, the monarch central complex is rotated by $\approx 90^{\circ}$ around the horizontal axis of the brain, reminiscent of the situation in *Manduca* and *Drosophila*. Consequently, the PB lies posteriorly (not dorsally), the noduli are ventrally located (not posteriorly), and the CBL lies anteriorly of the CBU (not ventrally). Both the CBL and the CBU consist of several horizontal layers in both species, with differences in the numbers of layers and their orientation

### *Lower division of the central body*

Compared with the six layers described in the locust CBL based on Bodian staining (Müller et al., 1997), only four layers have been revealed in the monarch CBL. As these were based on the analysis of projection areas originating from neurobiotin injections into the lateral triangle, they might not be fully comparable. However, as the neurobiotin fills originate from tangential neurons of the CBL (TL-neurons), we can propose initial homologies based on these cells. In the locust, five TL neurons have been described, three of which innervate specific CBL layers (Müller et al., 1997). In particular, layer 2 is selectively innervated by one type of polarization sensitive TL2 neuron in the locust, a situation comparable to the monarch (Heinze and Reppert, 2011). Additionally, layer 5 comprises a tube-like core of the locust CBL, innervated by TL3 neurons. Judged by its cylindrical shape and innervation by polarization sensitive tangential neurons resembling TL3 cells, layer 3 in the monarch is likely homolog to layer 5 of the locust. Although data about projection patterns of neurons innervating layers 1 and 4 of the monarch CBL is needed to reveal their still unknown counterparts in the locust, these comparisons already uncover a surprising degree of conservation between this structure in both species, despite their large evolutionary distance.

### *Upper division of the central body*

The monarch CBU appears more similar to the CBU (fan-shaped body) of flies and *Manduca* than to the CBU of the locust. The six layers in the monarch are linearly stacked from dorsal to ventral and roughly correspond to the eight layers of the *Drosophila* CBU (according to Young and Armstrong, 2010), with the ventral-most layer subdivided into three separate layers in the fly. The locust CBU appears more complex, as the three main layers are partly engulfing each other from anterior to posterior. With layers I and II being further subdivided into a dorsal and ventral compartment (Ia/b, IIa/b), and including the anterior lip as another CBU-associated structure, one counts also six compartments in the locust CBU (Homberg, 1991; Heinze and Homberg, 2008). Because of the extensive differences in orientation between the locust and monarch central complex, together with the different shape of individual layers, the CBU stratification is difficult to correlate between the two species. Nevertheless, as the distinction between the different strata and substrata in locusts was also based on serotonin-ir, and some serotonin-immunoreactivity tangential neurons appear to be conserved between lepidopterans and orthopterans (Homberg and Hildebrand, 1989; Homberg, 1991), the definition of strata in the monarch CBU might not only be a useful tool for mapping neuronal arborizations more reliably, but also provide initial evidence for homologies. However, the fact that no serotonin-immunoreactivity columnar neurons (layer III in locusts) are found in the monarch CBU shows the limitations of this

approach. Single-neuron morphologies are required to establish homologies on a broader basis.

### *Protocerebral bridge*

The discontinuous layout of the PB of the monarch is identical to the situation in *Manduca* (el Jundi et al., 2009) and is clearly different from other insects, including the locust and *Drosophila*. However, the two halves of the monarch PB are connected by a thick connective composed of tangential neurons that are very similar to those of the locust (Heinze and Reppert, 2011). Therefore, it remains to be shown whether the PB layout in the monarch and *Manduca* is a consequence of developmental constraints or has functional significance, as suggested for aquatic insects (Strausfeld, 1999). Underlining the potential functional similarity between the monarch PB and the locust PB, we described the posterior optic tubercle in the monarch with its connection to the PB, which clearly resembles the locust situation. Interestingly, to our knowledge, this appears to be the first report of the posterior optic tubercle in any lepidopteran insect. The locust posterior optic tubercle has also been proposed to mediate a second connection of the POL-network to the accessory medulla, suggesting a potential role of this neuropil for integrating circadian information in that species (el Jundi and Homberg, 2010).

Overall, the visual system of the monarch, including most neuropils associated with sun compass navigation, resembles the corresponding brain regions of *Manduca* and even flies more closely than that of locusts. Although some limited homologies can be established between the locust and the monarch, these data suggest that the brain layout at the level of neuropils is dictated by evolutionary links rather than migration behavior.

## Interspecies comparison of the olfactory system

### *Antennal lobes*

The monarch antennal lobe resembles that of other lepidopterans with respect to general shape, gross glomeruli number, location of cell groups, and distribution of GABA-ir (Hoskins et al., 1986; Berg et al., 2002; Huetteroth and Schachtner, 2005; Skiri et al., 2005; Berg et al., 2009; Kazawa et al., 2009). Unlike for moths, however, we did not detect sexual dimorphism of the antennal lobes, as those of males and females appeared to be identical. Based on location and size, we did identify two likely homologs of the sex-specific glomeruli of moths, which possessed identical features in both male and female monarchs. The remaining glomeruli were separated into several regions, as has been done for the commercial silkworm, *Bombyx mori* (Kazawa et al., 2009). As the fiber bundles and landmark glomeruli used for defining some of the regions in the antennal lobe of *Bombyx* were not identifiable in the monarch, we based the monarch glomerular groups solely on the shape and location of the glomeruli. Despite these differences, several regions seem to match between the two species. First, the anterior region covers the most anterior, readily identifiable glomeruli in both species; second, the posterior region consists of a number of large glomeruli with ambiguous boundaries as described also for other insects (Ignell et al., 2005), and the posterior dorsal region of the silkworm appears to cover similar glomeruli as in the monarch. The remaining regions of the silkworm, i.e., the anterior ventral, ventral, and anterior dorsal regions, are all included in the medial and posterior strata of the main group of ordinary, well-defined monarch glomeruli.

With the detailed description of the basic layout of the monarch antennal lobe, we provide an anatomical basis for analyzing interindividual variability, experience-dependent volumetric changes, and potential specializations of the olfactory system related to migration behavior.

### *Mushroom body*

When examining the general structure of the monarch mushroom body, two things stand out. First, the fused nature of the lobe system makes it impossible to separate the vertical and medial lobes with the methods used. To our knowledge, this fused system is unlike any insect mushroom body described yet, and leaves it to future work to define the identity of the different lobe structures with the help of single-cell morphologies. This finding is also unlike the schematic drawings of the monarch mushroom body lobes presented previously (Nordlander and Edwards, 1968). The second interesting feature of the monarch mushroom body is its clearly defined, complex double calyx, consisting of three separable subcompartments (inner-, outer-, and basal zones). This internal structure of the single calyces is different from moths (*Spodoptera littoralis, Manduca*), which only possess two concentrically arranged inner and outer zones but no basal zone (Homberg et al., 1988; Sjöholm et al., 2005, 2006). The monarch calyx layout is rather reminiscent of the honeybee calyx, which consists of a lip, collar, and basal ring (Strausfeld, 2002; Brandt et al., 2005). To establish homologies between the different compartments, mapping of sensory inputs will be important, as visual and olfactory inputs are clearly segregated in bees and other hymenopterans (Gronenberg, 2001).

A secondary lobe system, i.e., the Y-tract, has been described in lepidopterans before, containing either one or two loblets (Pearson, 1971; Homberg et al., 1988; Sjöholm et al., 2005). The location of the monarch Y-tract

components, including the dorsal and ventral loblets, is very similar to that of *Spodoptera* (Sjöholm et al., 2005). Considering the gross difference of the remaining lobes, this was surprising and underscores the independence of the two lobe systems.

In addition to the main calyx, an accessory calyx is present in many insect species. Like the primary calyx, this structure is also innervated by Kenyon cells, but fuses with the surrounding protocerebrum anteriorly. The location of the monarch accessory calyx on the ventral base of the primary calyces is identical to its location in *Manduca* (Homberg et al., 1988), although its size appears substantially reduced. In comparison, the accessory calyx of orthopterans is particularly large and receives gustatory tritocerebral input from the lobus glomerulatus (Weiss, 1981; Strausfeld et al., 2009). Considering the different neural connections and location relative to the primary calyx, it is unclear whether all structures collectively called accessory calyx are indeed homologous.

Volumetric comparison of the monarch mushroom body to the mushroom bodies of the available standard brains — *Drosophila* (Rein et al., 2002), the honeybee (Brandt et al., 2005), the locust (Kurylas et al., 2008), *Manduca* (el Jundi et al., 2009), *Tribolium* (Dreyer et al., 2010), the cockroach (Wei et al., 2010), and *Heliothis virescens* (Kvello et al., 2009) — reveals a similar volume (≈6%) as both moth species (*Manduca* and *H. virescens*) and *Drosophila* (relative to the sum of the medulla, lobula complex, central body, mushroom body, and antennal lobe), ranging from 5% in *H. virescens* to 7.5% in *Drosophila*. Much larger mushroom bodies are found in the honeybee (33%), the cockroach (33%), and *Tribolium* (24%), while the locust mushroom body size is in between (16%). More detailed comparison could be performed between the monarch and *Manduca*, as comparable reconstructions were performed. To omit the influence of the disproportionally enlarged monarch medulla, we compared mushroom body size relative to the central brain only for both species. We then find that the monarch mushroom body is nearly twice as large as that of *Manduca* (≈13.5% vs. 7.6% of the central brain). This is especially interesting because the primary olfactory centers, the antennal lobes, are more than 50% larger in *Manduca* (≈9.3% vs. 17% [males] or 14.7% [females] of the central brain). This suggests that a substantial portion of the mushroom body in the monarch is not involved in higher olfactory processing. Visual input into the calyx, potentially mediated by fiber bundles from the optic glomerular complex, could be processed in the monarch mushroom body. Substantial visual input to the calyx has so far only been shown in hymenopterans (Gronenberg, 2001), but evidence for dedicated regions of the calyx without olfactory input also exists in moths (Sjöholm et al., 2005).

## Unique aspects of the monarch brain

The majority of anatomical features identified in the monarch brain are also found in other insect species. However, some aspects of the monarch brain were unusual and may even be unique to the species. There were four neuropil areas that had not been described before: First, the optic glomerular complex, a large and brightly stained, presumably visual neuropil located in the optic stalk; second, the strap of the AOTu, a small neuropil linking the lower unit of the AOTu and the nodular unit of the AOTu; third, the anterior loblet of the LAL; and fourth, a small, elongated neuropil structure in the optic lobe, just anterior of the medulla (see Results for details). These regions are likely derivatives of known neuropils found in other insects, but their distinctive appearance suggests an increased importance of these structures in the monarch butterfly.

Two other monarch brain regions appeared to be substantially different from other insect brains: First, the upper unit of the AOTu was enlarged dramatically and reached a volume bigger than that of the central body. Second, the lobes of the mushroom body were fused almost completely into a homogeneous, spherical neuropil, so that none of the vertical or medial lobes were recognizable with the methods used. Which of these features are monarch-specific and which might be typical of butterflies in general will be resolved by studies of other butterflies.

## Toward a comprehensive understanding of the monarch brain

Other than by relative location, neuropil areas are characterized by their connections to other brain regions and their internal neuronal organization. Therefore, the most promising way toward a comprehensive map of the monarch brain that will enable us to draw conclusions about circuit function is to characterize the morphologies of individual neurons. The current atlas of the monarch brain neuropils provides the context for such an endeavor. A catalog of single neuron morphologies will reveal clear homologies between monarch neuropils and their counterparts in other species and highlight fundamental similarities among insect brains.

Additionally, a standardized monarch brain is needed to determine how unique the distribution of neuropil volumes in the monarch brain actually is and, importantly, whether there is a neuroanatomical substrate for the behavioral dimorphism between migratory and nonmigratory butterflies. Thus, volumetric and shape differences due to developmental and experiential changes will be illuminated and can also be compared with those in other species. Finally, a standardized monarch brain, together

with comparable studies in other migratory and nonmigratory insect species, will be essential for evaluating how evolutionary distance and lifestyle shape brain morphology and function.

## ACKNOWLEDGMENTS

We thank David G. Cook, Harlen E. Aschen, Altus Aschen, Carol Cullar, Fred Gagnon, and Edith Smith for catching or rearing monarch butterflies; Lauren Foley, Daniel Newman, Andrew Dowd, and Andrea Pereira for animal care; Christine Merlin for carrying out antennal backfills and assistance with monarch brain dissections; Scott Waddell for providing the anti-GABA antibody; and members of the Reppert lab for helpful discussions throughout the study.

## REFERENCES

Berg BG, Galizia CG, Brandt R, Mustaparta H. 2002. Digital atlases of the antennal lobe in two species of tobacco budworm moths, the Oriental *Helicoverpa assulta* (male) and the American *Heliothis virescens* (male and female). J Comp Neurol 446:123–134.

Berg BG, Schachtner J, Homberg U. 2009. Gamma-aminobutyric acid immunostaining in the antennal lobe of the moth *Heliothis virescens* and its colocalization with neuropeptides. Cell Tissue Res 335:593–605.

Brandt R, Rohlfing T, Rybak J, Krofczik S, Maye A, Westerhoff M, Hege H-C, Menzel R. 2005. Three-dimensional average-shape atlas of the honeybee brain and its applications. J Comp Neurol 492:1–19.

Dacks AM, Christensen TA, Hildebrand JG. 2006. Phylogeny of a serotonin-immunoreactive neuron in the primary olfactory center of the insect brain. J Comp Neurol 498:727–746.

Dickens J, Eaton J. 1973. External ocelli in Lepidoptera previously considered to be anocellate. Nature 242:205–206.

Dreyer D, Vitt H, Dippel S, Goetz B, el Jundi B, Kollmann M, Huetteroth W, Schachtner J. 2010. 3D standard brain of the red flour beetle *Tribolium castaneum*: a tool to study metamorphic development and adult plasticity. Front Syst Neurosci 4:3.

el Jundi B, Homberg U. 2010. Evidence for the possible existence of a second polarization-vision pathway in the locust brain. J Insect Physiol 56:971–979.

el Jundi B, Huetteroth W, Kurylas AE, Schachtner J. 2009. Anisometric brain dimorphism revisited: implementation of a volumetric 3D standard brain in *Manduca sexta*. J Comp Neurol 517:210–225.

Fischbach KF, Dittrich APM. 1989. The optic lobe of *Drosophila melanogaster*. I: A. Golgi analysis of wild-type structure. Cell Tissue Res 258:441–475.

Froy O, Gotter AL, Casselman AL, Reppert SM. 2003. Illuminating the circadian clock in monarch butterfly migration. Science 300:1303–1305.

Gronenberg W. 2001. Subdivisions of hymenopteran mushroom body calyces by their afferent supply. J Comp Neurol 435:474–489.

Gronenberg W, Hölldobler B. 1999. Morphologic representation of visual and antennal information in the ant brain. J Comp Neurol 412:229–240.

Hanesch U, Fischbach KF, Heisenberg M. 1989. Neuronal architecture of the central complex in *Drosophila melanogaster*. Cell Tissue Res 257:343–366.

Heinze S, Homberg U. 2007. Maplike representation of celestial E-vector orientations in the brain of an insect. Science 315:995–997.

Heinze S, Homberg U. 2008. Neuroarchitecture of the central complex of the desert locust: intrinsic and columnar neurons. J Comp Neurol 511:454–478.

Heinze S, Reppert SM. 2011. Sun compass integration of skylight cues in migratory monarch butterflies. Neuron 69: 345–358.

Heinze S, Gotthardt S, Homberg U. 2009. Transformation of polarized light information in the central complex of the locust. J Neurosci 29:11783–11793.

Homberg U. 1991. Neuroarchitecture of the central complex in the brain of the locust *Schistocerca gregaria* and *S. americana* as revealed by serotonin immunocytochemistry. J Comp Neurol 303:245–254.

Homberg U. 2004. In search of the sky compass in the insect brain. Naturwissenschaften 91:199–208.

Homberg U. 2008. Evolution of the central complex in the arthropod brain with respect to the visual system. Arthropod Struct Dev 37:347–362.

Homberg U, Hildebrand JG. 1989. Serotonin-immunoreactive neurons in the median protocerebrum and suboesophageal ganglion of the sphinx moth *Manduca sexta*. Cell Tissue Res 258:1–24.

Homberg U, Paech A. 2002. Ultrastructure and orientation of ommatidia in the dorsal rim area of the locust compound eye. Arthropod Struct Dev 30:271–280.

Homberg U, Kingan TG, Hildebrand JG. 1987. Immunocytochemistry of GABA in the brain and suboesophageal ganglion of *Manduca sexta*. Cell Tissue Res 248:1–24.

Homberg U, Montague RA, Hildebrand JG. 1988. Anatomy of antenno-cerebral pathways in the brain of the sphinx moth *Manduca sexta*. Cell Tissue Res 254:255–281.

Homberg U, Würden S, Dircksen H, Rao K. 1991. Comparative anatomy of pigment-dispersing hormone-immunoreactive neurons in the brain of orthopteroid insects. Cell Tissue Res 266:343–357.

Homberg U, Vitzthum H, Müller M, Binkle U. 1999. Immunocytochemistry of GABA in the central complex of the locust *Schistocerca gregaria*: identification of immunoreactive neurons and colocalization with neuropeptides. J Comp Neurol 409:495–507.

Homberg U, Hofer S, Pfeiffer K, Gebhardt S. 2003. Organization and neural connections of the anterior optic tubercle in the brain of the locust, *Schistocerca gregaria*. J Comp Neurol 462:415–430.

Homberg U, Heinze S, Pfeiffer K, Kinoshita M, el Jundi B. 2011. Central neural coding of sky polarization in insects. Philos Trans R Soc Lond B Biol Sci 366:680–687.

Hoskins SG, Homberg U, Kingan TG, Christensen TA, Hildebrand JG. 1986. Immunocytochemistry of GABA in the antennal lobes of the sphinx moth *Manduca sexta*. Cell Tissue Res 244:243–252.

Huetteroth W, Schachtner J. 2005. Standard three-dimensional glomeruli of the *Manduca sexta* antennal lobe: a tool to study both developmental and adult neuronal plasticity. Cell Tissue Res 319:513–524.

Huetteroth W, el Jundi B, el Jundi S, Schachtner J. 2010. Frontiers: 3D-reconstructions and virtual 4D-visualization to study metamorphic brain development in the sphinx moth *Manduca sexta*. Front Syst Neurosci 4:7.

Ignell R, Dekker T, Ghaninia M. 2005. Neuronal architecture of the mosquito deutocerebrum. J Comp Neurol 493:207–240.

Iwano M, Hill ES, Mori A, Mishima T, Mishima T, Ito K, Kanzaki R. 2010. Neurons associated with the flip-flop activity in the lateral accessory lobe and ventral protocerebrum of the silkworm moth brain. J Comp Neurol 518:366–388.

Kazawa T, Namiki S, Fukushima R, Terada M, Soo K, Kanzaki R. 2009. Constancy and variability of glomerular organization in the antennal lobe of the silkmoth. Cell Tissue Res 336:119–136.

Klagges BR, Heimbeck G, Godenschwege TA, Hofbauer A, Pflugfelder GO, Reifegerste R, Reisch D, Schaupp M, Buchner S, Buchner E. 1996. Invertebrate synapsins: a single gene codes for several isoforms in *Drosophila*. J Neurosci 16:3154–3165.

Kurylas AE, Rohlfing T, Krofczik S, Jenett A, Homberg U. 2008. Standardized atlas of the brain of the desert locust, *Schistocerca gregaria*. Cell Tissue Res 333:125–145.

Kvello P, Løfaldli BB, Rybak J, Menzel R, Mustaparta H. 2009. Digital, three-dimensional average shaped atlas of the *Heliothis virescens* brain with integrated gustatory and olfactory neurons. Front Syst Neurosci 3:14.

Labhart T, Meyer EP. 1999. Detectors for polarized skylight in insects: a survey of ommatidial specializations in the dorsal rim area of the compound eye. Microsc Res Tech 47: 368–379.

Labhart T, Baumann F, Bernard GD. 2009. Specialized ommatidia of the polarization-sensitive dorsal rim area in the eye of monarch butterflies have non-functional reflecting tapeta. Cell Tissue Res 338:391–400.

Merlin C, Gegear RJ, Reppert SM. 2009. Antennal circadian clocks coordinate sun compass orientation in migratory monarch butterflies. Science 325:1700–1704.

Mota T, Yamagata N, Giurfa M, Gronenberg W, Sandoz JC. 2011. Neural organization and visual processing in the anterior optic tubercle of the honeybee brain. J Neurosci 31: 11443–11456.

Mouritsen H, Frost BJ. 2002. Virtual migration in tethered flying monarch butterflies reveals their orientation mechanisms. Proc Natl Acad Sci U S A 99:10162–10166.

Müller M, Homberg U, Kühn A. 1997. Neuroarchitecture of the lower division of the central body in the brain of the locust (*Schistocerca gregaria*). Cell Tissue Res 288: 159–176.

Nordlander RH, Edwards JS. 1968. Morphology of the larval and adult brains of the monarch butterfly, *Danaus plexippus plexippus, L*. J Morphol 126:67–94.

Otsuna H, Ito K. 2006. Systematic analysis of the visual projection neurons of *Drosophila melanogaster*. I. Lobula-specific pathways. J Comp Neurol 497:928–958.

Ott SR. 2008. Confocal microscopy in large insect brains: zinc-formaldehyde fixation improves synapsin immunostaining and preservation of morphology in whole-mounts. J Neurosci Methods 172:220–230.

Pearson L. 1971. The corpora pedunculata of *Sphinx ligustri L*. and other Lepidoptera — an anatomical study. Philos Trans R Soc Lond B Biol Sci 259:477–516.

Perez S, Taylor O, Jander R. 1997. A sun compass in monarch butterflies. Nature 387:29–29.

Pfeiffer K, Homberg U. 2007. Coding of azimuthal directions via time-compensated combination of celestial compass cues. Curr Biol 17:960–965.

Pfeiffer K, Kinoshita M. 2012. Segregation of visual inputs from different regions of the compound eye in two parallel pathways through the anterior optic tubercle of the bumblebee (*Bombus ignitus*). J Comp Neurol 520:212–219.

Pfeiffer K, Kinoshita M, Homberg U. 2005. Polarization-sensitive and light-sensitive neurons in two parallel pathways passing through the anterior optic tubercle in the locust brain. J Neurophys 94:3903–3915.

Rein K, Zöckler M, Mader MT, Grübel C, Heisenberg M. 2002. The *Drosophila* standard brain. Curr Biol 12:227–231.

Reppert SM. 2006. A colorful model of the circadian clock. Cell 124:233–236.

Reppert SM, Zhu H, White RH. 2004. Polarized light helps monarch butterflies navigate. Curr Biol 14:155–158.

Reppert SM, Gegear RJ, Merlin C. 2010. Navigational mechanisms of migrating monarch butterflies. Trends Neurosci 33:399–406.

Sakura M, Lambrinos D, Labhart T. 2008. Polarized skylight navigation in insects: model and electrophysiology of e-vector coding by neurons in the central complex. J Neurophys 99:667–682.

Sauman I, Briscoe AD, Zhu H, Shi D, Froy O, Stalleicken J, Yuan Q, Casselman A, Reppert SM. 2005. Connecting the navigational clock to sun compass input in monarch butterfly brain. Neuron 46:457–467.

Schildberger K. 1983. Local interneurons associated with the mushroom bodies and the central body in the brain of *Acheta domesticus*. Cell Tissue Res 230:573–586.

Sjöholm M, Sinakevitch I, Ignell R, Strausfeld NJ, Hansson BS. 2005. Organization of Kenyon cells in subdivisions of the mushroom bodies of a lepidopteran insect. J Comp Neurol 491:290–304.

Sjöholm M, Sinakevitch I, Strausfeld NJ, Ignell R, Hansson BS. 2006. Functional division of intrinsic neurons in the mushroom bodies of male *Spodoptera littoralis* revealed by antibodies against aspartate, taurine, FMRF-amide, Mas-allatotropin and DC0. Arthropod Struct Dev 35: 153–168.

Skiri HT, Rø H, Berg BG, Mustaparta H. 2005. Consistent organization of glomeruli in the antennal lobes of related species of heliothine moths. J Comp Neurol 491: 367–380.

Stalleicken J, Labhart T, Mouritsen H. 2006. Physiological characterization of the compound eye in monarch butterflies with focus on the dorsal rim area. J Comp Physiol A 192:321–331.

Strausfeld NJ. 1970. Golgi studies on insects. Part II. The optic lobes of diptera. Philos Trans R Soc Lond B Biol Sci 258:135–223.

Strausfeld NJ. 1976. Atlas of an insect brain. New York: Springer.

Strausfeld NJ. 1999. A brain region in insects that supervises walking. Prog Brain Res 123:273–284.

Strausfeld NJ. 2002. Organization of the honey bee mushroom body: representation of the calyx within the vertical and gamma lobes. J Comp Neurol 450:4–33.

Strausfeld N, Blest AD. 1970. Golgi studies on insects. Part I. The optic lobes of Lepidoptera. Philos Trans R Soc Lond B Biol Sci 258:81–134.

Strausfeld NJ, Sinakevitch I, Brown SM, Farris SM. 2009. Ground plan of the insect mushroom body: functional and evolutionary implications. J Comp Neurol 513:265–291.

Strauss R. 2002. The central complex and the genetic dissection of locomotor behaviour. Curr Opin Neurobiol 12: 633–638.

Vitzthum H, Müller M, Homberg U. 2002. Neurons of the central complex of the locust *Schistocerca gregaria* are sensitive to polarized light. J Neurosci 22:1114–1125.

Wei H, el Jundi B, Homberg U, Stengl M. 2010. Implementation of pigment-dispersing factor-immunoreactive neurons in a standardized atlas of the brain of the cockroach *Leucophaea maderae*. J Comp Neurol 518:4113–4133.

Weiss MJ. 1981. Structural patterns in the corpora pedunculata of orthoptera: a reduced silver analysis. J Comp Neurol 203:515–553.

Wendt B, Homberg U. 1992. Immunocytochemistry of dopamine in the brain of the locust *Schistocerca gregaria*. J Comp Neurol 321:387–403.

Williams JLD. 1975. Anatomical studies of the insect central nervous system: a ground-plan of the midbrain and an

introduction to the central complex in the locust, *Schistocerca gregaria* (Orthoptera). J Zool 176:67–86.

Young JM, Armstrong J. 2010. Structure of the adult central complex in *Drosophila*: organization of distinct neuronal subsets. J Comp Neurol 518:1500–1524.

Zhan S, Merlin C, Boore JL, Reppert SM. 2011. The monarch butterfly genome yields insights into long-distance migration. Cell 147:1171–1185.

Zhu H, Casselman AL, Reppert SM. 2008. Chasing migration genes: a brain expressed sequence tag resource for summer and migratory monarch butterflies (*Danaus plexippus*). PLoS ONE 3:e1345.

Zhu H, Gegear RJ, Casselman AL, Kanginakudru S, Reppert SM. 2009. Defining behavioral and molecular differences between summer and migratory monarch butterflies. BMC Biol 7:14.